Testing spectral models for stellar populations with star clusters: II. Results

Rosa M. González Delgado[1][*] and Roberto Cid Fernandes[2]†

[1] *Instituto de Astrofísica de Andalucía (CSIC), P.O. Box 3004, 18080 GRANADA, Spain*
[2] *Departamento de Física-CFM, Universidade Federal de Santa Catarina, C.P.. 476, 88040-900, Florianópolis, SC, Brazil*

2009 July

ABSTRACT
High spectral resolution evolutionary synthesis models have become a routinely used ingredient in extragalactic work, and as such deserve thorough testing. Star clusters are ideal laboratories for such tests. This paper applies the spectral fitting methodology outlined in Paper I to a sample of clusters, mainly from the Magellanic Clouds and spanning a wide range in age and metallicity, fitting their integrated light spectra with a suite of modern evolutionary synthesis models for single stellar population. The combinations of model plus spectral library employed in this investigation are Galaxev/STELIB, Vazdekis/MILES, SED@/GRANADA, and Galaxev/MILES+GRANADA, which provide a representative sample of models currently available for spectral fitting work. A series of empirical tests are performed with these models, comparing the quality of the spectral fits and the values of age, metallicity and extinction obtained with each of them. A comparison is also made between the properties derived from these spectral fits and literature data on these nearby, well studied clusters. These comparisons are done with the general goal of providing useful feedback for model makers, as well as guidance to the users of such models. We find that: (1) All models are able to derive ages that are in good agreement both with each other and with literature data, although ages derived from spectral fits are on average slightly older than those based on the S-CMD method as calibrated by Girardi et al. (1995). (2) There is less agreement between the models for the metallicity and extinction. In particular, Galaxev/STELIB models underestimate the metallicity by ∼0.6 dex, and the extinction is overestimated by 0.1 mag. (3) New generation of models using the GRANADA and MILES libraries are superior to STELIB-based models both in terms of spectral fit quality and regarding the accuracy with which age and metallicity are retrieved. Accuracies of about 0.1 dex in age and 0.3 dex in metallicity can be achieved as long as the models are not extrapolated beyond their expected range of validity.

Key words: techniques: spectroscopic – galaxies: Stellar populations–galaxies: star clusters–Magellanic Clouds

1 INTRODUCTION

Evolutionary synthesis has progressed significantly since this technique was introduced by Tinsley (1968). In particular, high/intermediate spectral resolution stellar libraries like STELIB (Le Borgne et al. 2003), INDO-US (Valdes et al. 2004), ELODIE (Prugniel & Soubiran 2004), GRANADA (Martins et al. 2005); INAOE (Rodríguez-Merino et al. 2005), and MILES (Sánchez-Blázquez et al. 2006) have been incorporated into evolutionary synthesis codes (e.g. Bruzual

& Charlot 2003, hereafter BC03; Le Borgne et al. 2004; González Delgado et al. 2005) whose predictions are now routinely used in the analysis of galaxy spectra. With the proliferation of evolutionary synthesis models, it becomes critically important to test them, specially in light of the fact that a enormous fraction of extragalactic studies are heavily dependent on them.

Because of their complex mixture of stellar populations, galaxies are not ideal test beds for evolutionary synthesis models. Star clusters (SCs), on the other hand, are suitable laboratories for this purpose. Presumably formed in a single burst, SCs can be characterized by a single age (t), a single metallicity (Z), and an extinction (A_V). Even taking into

[*] E-mail: rosa@iaa.es
† E-mail:cid@astro.ufsc.br

account caveats like stochastic effects (Cerviño et al. 2002; Maíz-Apellániz 2009) and the possibility of non-unique populations (e.g. NGC 1569, González Delgado et al. 1997; and ω Cen, Meylan 2003), SCs are by far and large the simplest systems available to test evolutionary synthesis models. Furthermore, SC properties can be determined from spatially resolved observations like color-magnitude diagrams (CMD) and spectroscopy of individual stars, providing a benchmark for empirical tests of integrated light models. SC integrated light, through colors or spectra, have also been very useful to test stellar population models, in particular the clusters in the Magellanic Clouds (e.g. Beasley et al. 2002; de Grijs & Anders 2006; Pessev et al. 2008; Santos et al. 2006).

Studies in this general vein have been carried out in the last couple of years. Wolf et al (2007) fitted low resolution spectra of SCs using the BC03 models, finding ages and metallicities in good agreement with independent estimates for ages > 1 Gyr. For younger clusters the agreement in ages is still acceptable (0.3 dex), but metallicities cannot be well constrained. More recently, Koleva et al. (2008) have fitted high resolution spectra of SCs with STELIB, MILES and ELODIE based models. Results for the latter two libraries are consistent with each other and with ages and metallicities derived from spatially resolved studies, while the BC03 STELIB based models produce discrepancies associated with the incompleteness of this library, specially in metallicity. Their results validate full spectral fitting as a means to estimate SC properties, while at the same time highlighting the importance of stellar libraries in this game.

This paper follows this same general direction. We present results of a λ-by-λ spectral synthesis analysis of SCs obtained with different sets of high resolution evolutionary synthesis models. The main differences between this study and that by Wolf et al. (2007) are that they focus on only one set of BC03 models, and use data covering a wider wavelength interval but at coarser spectral resolution than the one used here. Compared to Koleva et al. (2008), our study differs mostly in the properties of the target SCs. Our sample is composed mainly of young and intermediate age SCs in the Large and Small Magellanic Clouds (LMC and SMC, respectively), whereas Koleva et al. concentrate on an older population of Galactic globular clusters. There also differences in the fitting methodology, like the fact that our fits do take into account the continuum shape, whereas these two studies apply spectral rectification techniques. Together, these complementary approaches provide valuable feedback to evolutionary synthesis modelers, as well as guidance to users of these models.

This study started in Paper I (Cid Fernandes & González Delgado 2009), where we presented our spectral fitting methodology. High quality spectra in the 3650–4600 Å range of 27 SCs from the sample of Leonardi & Rose (2003, hereafter LR03), were fitted with single stellar population (SSP) spectral models from Vazdekis et al. (2009), based on the MILES library. The fits were carried out with the publicly available STARLIGHT code (Cid Fernandes et al. 2005, 2008), never before used for SC work. Covariance maps and a simple bayesian parameter estimation formalism were also presented. In this second paper, the same methodology is extended to other publicly available high resolution evolutionary models. The results are compared both among themselves and to independent estimates of t and Z. This

allows us to (1) compare the quality of spectral fits obtained with different models, (2) quantify uncertainties and biases in SC properties resulting from differences between different models, and (3) check the reliability of the ages and metallicities derived from detailed spectral fitting as compared to more traditional methods [1].

This study can be looked at from two different perspectives: (a) Validation of spectral fitting as a means of inferring the properties of SCs, or (b) validation of evolutionary synthesis models for use in extragalactic work. Our main interest is in the latter, and this influences the way we present our results, but researchers more interested in SCs per se can also benefit from this study.

The SC sample and information about the age, metallicity, and extinction previously reported in the literature are described in Section 2. The seven SSP models used here come from four sources: BC03, Charlot &Bruzual (2009, in preparation), González Delgado et al (2005), and Vazdekis et al. (2009). Section 3 presents a brief description of each of these. Results start in Section 4, where we compare the quality of spectral fits obtained with different models. Section 5 compares SC properties derived with different models, whereas in Section 6 we compare the results obtained with spectral synthesis to those previously obtained from CMD, broad band colors, or spectral indices. The discussion is presented in Section 7. Section 8 summarizes our main conclusions.

2   THE SAMPLE AND LITERATURE DATA

The sample analyzed here comprises the same 27 SCs from LR03 studied in Paper I, 20 of which are from the LMC, while 3 belong to the SMC and 4 are Galactic clusters. The spectra cover the 3650–4600 Å wavelength range with a typical S/N of about 50. This spectral range is very suitable for testing models at young and intermediate ages because it covers the Balmer jump and the high-order Balmer series (González Delgado et al. 1999).

The LMC SCs which dominate this sample were originally selected by LR03 from Sagar & Pandey (1989), who compiled the ages and metallicities derived from CMDs in the literature. These SCs cover the well known range of ages and metallicities in the LMC, reflecting the age-metallicity gap in that galaxy (e.g. Girardi et al. 1995). Thus, most of them are younger than 2 Gyr (age interval is between 30 Myr and 2 Gyr), with metallicities over 0.25 solar, while a few are old and very metal poor. To extend the analysis to the low metallicity and old age regime, 3 SCs from the SMC (NGC 411, NGC 416 and NGC 419) and 4 from the Galaxy (47 Tuc, M15, M79 and NGC 1851) are included in the sample. These extra SCs approximately cover the t-Z gap of the LMC SCs.

Fiducial reference values of t and Z determined from fundamental methods are required for comparison with our spectral fitting estimates [2]. CMD based ages should be the

---

[1] We are not able to derive the photometric mass of each cluster because, even though the spectra are flux calibrated, the absolute scale is unknown.
[2] We will refer to our results as "STARLIGHT" or "spectral fitting" ages, metallicities, and extinctions.

best option. However, due to the lack of consistency and homogeneity of the results based on the CMDs, we adopted the values tabulated by LR03.

LR03 adopted ages which are derived from a secondary indicator, the S parameter, based on $U - B$ and $B - V$ integrated colors. The S parameter provides an empirical relation between the age of a SC and its integrated colors (Elson & Fall 1989). LR03 use UBV photometry from Bica et al. (1992, 1996) and the S parameter calibration given by Girardi et al. (1995), based on 24 LMC clusters whose ages are estimated from high-quality ground-based CMDs. Note, however, that this relation between S and $\log t$ has a rms dispersion of 0.137 dex. For metallicities we have also adopted the value given in LR03, taken from Olszewski et al. (1991) and based on the equivalent width of the CaII triplet at 8500 Å as measured in one or several stars of each SC, and from the compilations from Seggewiss & Richtler (1989), and Sagar & Pandey (1989). These ages and metallicities are listed in columns 3 and 4 of Table 1. We will take these values as reference for the results of our spectral fitting estimates of t and Z.

Table 1 also lists the ages and metallicities derived by LR03 using the Balmer discontinuity, and two absorption indices based on Hδ/FeIλ4045, and CaII H+Hϵ/CaII K line ratios. LR03 found a good correlation between their results and those from the Girardi et al. (1995) calibration, but their ages are about 50% older. The correlation between the index-based metallicities of LR03 and those from the CaII triplet are worse, presenting a large scatter as well as a systematic offset, with the L03 metallicities systematically smaller than those of Olszewski et al. (1991). Table 1 also lists ages and metallicities from CMD analysis, taken from a variety of sources. For the four Galactic clusters of this sample, we have taken the data from the work of Koleva et al. (2008) derived from full spectral fitting, but Table 1 also quotes the metallicities compiled by Schiavon et al. (2005) for the same SCs. The comparison of these two sets of values provides a rough estimation of the uncertainties on the literature metallicity for these four old clusters.

Finally, we have compiled the V-band extinction A_V from the literature. Bica & Alloin (1986) give a global extinction towards the LMC and SMC that is $A_V \leqslant 0.2$ and 0.1, respectively. McLaughling & van der Marel (2005) use the BC03 models and optical colors to derive the V-band mass to light ratios and reddening. The A_V values obtained are also low, ranging between 0.03 and 0.09, with a mean 0.06 for the SCs of this sample. Pessev et al. (2008) gives the extinction obtained using the web tool by the Magellanic Clouds Photometric Survey (MCPS, Zaritsky, Harris & Thompson 1997; Zaritsky et al. 2004), which gives A_V estimates along the line-of-sight to stars within a search radius of the SC coordinates. These estimates range between $A_V = 0.17$ and 0.76, with a mean value of 0.35. This method can only provide a rough estimate of the extinction. Pessev et al. (2008) also compile the extinction for 9 of the SCs of the sample estimated from CMDs, A_V ranges between 0.03 and 0.37. The last columns of Table 1 summarize these estimates.

3 EVOLUTIONARY SYNTHESIS MODELS

Evolutionary tracks and stellar libraries are the two most important ingredients in evolutionary synthesis models. Stellar libraries, in particular, have been the subject of many independent studies over the past five years. Several groups have put a lot of effort towards building complete stellar libraries at high/intermediate spectral resolution, mainly at optical wavelengths (see e.g. the review by González Delgado 2009). As a result of these efforts, there are nowadays several sets of models available for spectral synthesis work.

From a neutral user perspective, it is not at all obvious which set of models should be adopted. Since one of the main goals of this paper is precisely to evaluate the impact of this choice, we fit each of our SC spectra with models from four different publicly available sources, out of which a total of 7128 SSP spectra were retrieved. We are particularly interested in evaluating the effects of the spectral libraries, but the chosen models also differ in evolutionary tracks, IMF and "model-maker" (i.e., the evolutionary synthesis code which combines these ingredients to produce SSP spectra). While non-exhaustive, this large set is highly representative of the options currently available to model users.

In what follows we briefly describe each of these sets of models. A summary of these models is given in Table 2.

3.1 Galaxev and STELIB

STELIB[3] is an empirical library that contains 249 stellar spectra in the 3200–9500 Å range with a spectral resolution of 3 Å (Le Borgne et al. 2003). There are 84 stars at solar metallicity, 42 stars are oversolar and 69 stars around half solar and only 23 and 18 stars with metallicity in the intervals 0.1–0.3, and 0.01–0.1 solar, respectively. The library lacks hot (over 10000 K), metal-rich, and cool dwarf stars.

Galaxev[4] (BC03) computes the evolutionary synthesis models with two assumptions for the IMF: Salpeter and Chabrier (Chabrier 2003), both between 0.1 and 100 $M_\odot$. Two sets of evolutionary models are used, one with the Padova 1994 (Bertelli et al. 1994) and the other with Padova 2000 (Girardi et al. 2000, 2002) isochrones. The 1994 isochrones are recommended by BC03, on the basis that the 2000 isochrones produce red giant branches that are 50–200 K hotter than Padova 1994, and in consequence they yield older ages for elliptical galaxies.

The SSP spectra are distributed in 221 ages ($0 \leqslant t \leqslant 20$ Gyr) and 6 metallicities ($0.0001 \leqslant Z \leqslant 0.05$ for Padova 1994 and $0.0004 \leqslant Z \leqslant 0.03$ for Padova 2000). Note that the results obtained with Galaxev+STELIB models at low and high metallicities are limited by the low number of stars at $Z \leqslant 0.004$ and the lack of metal rich giant stars (see BC03). For SSPs older than 100 Myr and Z between 0.2 solar and solar, these models can produce accurate predictions.

3.2 SED@ and the GRANADA stellar library

The GRANADA library[5] (Martins et al. 2005) contains 1654 high spectral resolution stellar spectra with a sam-

Name	ID	log age (yr) S	[Fe/H]	log age (yr) Indices	[Fe/H] Indices	log age (yr) CMD	[Fe/H] CMD	Ref.	A_V CMD	A_V MCPS	A_V McL
(1)	(2)	(3)	(4)	(5)	(6)	(7)	(8)	(9)	(10)	(11)	(12)
NGC411	1	9.25	-0.84	9.09	-0.43				0.37	0.17	
NGC416	2	9.84	-1.44	9.82	-1.27				0.25	0.20	
NGC419	3	9.08	-0.70	9.22	-0.90					0.20	
NGC1651	4	9.20	-0.37	9.34	-0.82	9.30	-0.70	Ke07	0.34	0.35	0.03
						9.30		Ge97			
NGC1754	5	10.2	-1.42	9.74	-1.44	10.19		Ol98	0.28	0.40	0.05
NGC1783	6	8.94	-0.75	9.19	-0.54	9.11		Ge97		0.30	
NGC1795	7	9.23	-0.23	9.30	-0.69	9.23		Ge97			
NGC1806	8	8.70	-0.23	9.28	-0.64					0.25	
NGC1818	9	7.54	-0.90	7.30						0.39	0.05
NGC1831	10	8.57	0.010	8.70	-0.65	8.60	0.01	Gi95	0.34	0.39	0.04
						8.85	-0.01	Ke07			
NGC1846	11	9.09	-0.70	9.50	-1.40					0.41	
NGC1866	12	8.34	-1.20	8.48		8.14	-0.4:	Gi95		0.28	0.03
NGC1978	13	9.23	-0.42	9.41	-0.72	9.3		Ge97		0.76	
NGC2010	14	8.20	0.00	7.92		8.19	-0.4:	Gi95			
NGC2133	15	8.11	-1.00	8.16							
NGC2134	16	8.28	-1.00	8.80		8.15	-0.4:	Gi95		0.62	
NGC2136	17	8.04	-0.40	7.91		8.00	-0.55	Di00		0.58	0.09
NGC2203	18	9.26	-0.52	9.19	-0.46	9.25		Ge97		0.39	
NGC2210	19	10.1	-1.97	9.58	-1.16	10.2		Ge97	0.28	0.39	0.03
NGC2213	20	9.01	-0.01	9.32	-0.88	9.23	-0.70	Ke07	0.19	0.40	0.08
						9.20		Ge97			
NGC2214	21	7.91	-1.20	7.72		7.92	-0.4:	Gi95		0.39	0.09
NGC2249	22	8.72	-0.05	8.44	-0.40	8.54	-0.4	Gi95	0.03	0.39	0.06
						9.0	-0.45	Ke07			
NGC2121	23					9.46	-0.40	Ke07	0.22	0.53	0.10
						9.3		Ge97			
47Tuc	24			10.1	-0.76, -0.70*						
M15	25			10.0	-2.29						
M79	26			10.1	-1.95, -1.55*						
NGC1851	27			9.72	-1.16, -1.21*						

Table 1. Properties (age, metallicity and extinction) of the SCs from the literature. Col. (1): SC name. Col. (2): SC ID number. Col. (3): Ages derived using the S-parameter from Girardi et al. (1995) and tabulated by LR03. Col. (4): Metallicity obtained with the equivalent width of the CaII triplet from Olszewski et al. (1991), and compilation by Seggewiss & Richtler (1989), and Sagar & Pandey (1989). Col. (5) and (6): Ages and metallicities obtained by LR03 using the CaII and Hδ/Fe indices for the SMC and LMC SCs. The data for the four Galactic clusters are from the spectral fitting technique by Koleva et al. (2008). Metallicities from Schiavon et al. (2005) for three of these GC are marked by "*". Col. (7) and (8): Ages and metallicities obtained from CMD studies. Col. (9): References for Col. 7 and 8. Ke07: Kerber et al. (2007); Ge97: Geisler et al. (1997); Ol98: Olsen et al. (1998); Gi95: Girardi et al. (1995); Di00: Dirsch et al. (2000). Col. (10), and Col. (11): Extinctions derived from CMD studies, Magellanic Clouds Photometric Surveys (MCPS), respectively, tabulated by Pessev et al. (2008). Col. (12): Extinctions values from McLaughlin & van der Marel (2005).

pling of 0.3 Å covering from 3000 to 7000 Å. The spectra were computed for a wide range of effective temperatures ($3000 \leqslant T_{\text{eff}} \leqslant 55000$ K), and gravity ($-0.5 \leqslant \log g \leqslant 5.5$), and four metallicities (0.1, 0.5, 1 and 2 solar). The most up-to-date stellar atmosphere models were used: a) the non-LTE line blanketed models from Lanz & Hubeny (2003) for hot stars ($T_{\text{eff}} \geqslant 27500$ K); b) ATLAS9 models (Kurucz 1993) for intermediate temperature stars (4500–27000 K); and c) PHOENIX LTE line blanketed models (Hauschildt & Baron 1999) for cool stars (3000–4500 K). High resolution synthetic spectra were obtained with the programs SYN-THE and ROT by Hubeny, Lanz & Jeffery (1995).

The library was implemented in SED@[6] (Cerviño & Luridiana 2006) to predict SSP spectra using the non-rotating Geneva tracks including standard mass-loss rates

and the Padova tracks (González Delgado et al. 2005). Here, however, we use only the models generated with the Padova 2000 isochrones (Girardi et al. 2000, 2002). The IMF is assumed to be that of Salpeter (1955) between 0.1 and 120 $M_\odot$. SSP models for 3 metallicities (0.004, 0.008 and 0.019), and 74 ages between 4 Myr and 17.78 Gyr are available.

3.3 Vazdekis-MILES

The MILES library contains about one thousand stars spanning a large range of stellar parameters (Sánchez-Blázquez et al. 2006). The spectra were taken at the Isaac Newton Telescope in the Roque de Los Muchachos Observatory at La Palma, covering the range from 3500 to 7500 Å at a resolution of 2.3 Å (FWHM). This library represents a significant improvement with respect to STELIB in the coverage of metallicity, number of giant stars and other aspects, such

[6] http://www.iaa.csic.es/~mcs/sed@

Table 2. Sets of SSP models used for spectral fitting

Model-set		Code	Isochrones	IMF	Library	N_Z	Metallicities	N_t	Ages [Gyr]
BC00s	-1	Galaxev	Padova2000	Salpeter	STELIB	6	0.03, 0.019, 0.008, 0.004, 0.001, 0.0004	221	0–20
BC00c	+1	Galaxev	Padova2000	Chabrier	STELIB	6	0.03, 0.019, 0.008, 0.004, 0.001, 0.0004	221	0–20
BC94s	-2	Galaxev	Padova1994	Salpeter	STELIB	6	0.05, 0.02, 0.008, 0.004, 0.0004, 0.0001	221	0–20
BC94c	+2	Galaxev	Padova1994	Chabrier	STELIB	6	0.05, 0.02, 0.008, 0.004, 0.0004, 0.0001	221	0–20
CB94c	+3	Galaxev	Padova1994	Chabrier	MILES	6	0.05, 0.02, 0.008, 0.004, 0.0004, 0.0001	221	0–20
RG00s	+4	SED@	Padova2000	Salpeter	GRANADA	3	0.019, 0.008, 0.004	74	0.004–17.78
V00s	+5	Vazdekis	Padova2000	Salpeter	MILES	6	0.03, 0.019, 0.008, 0.004, 0.001, 0.0004	46	0.1–17.78

as flux and wavelength calibrations. However, MILES has still only a small number of hot (> 15000 K) stars.

This library was incorporated into the evolutionary synthesis code of Vazdekis (1999). SSP spectra[7] using the Padova 2000 tracks and Salpeter IMF were computed for 6 metallicities in the 0.0004–0.03 range, and 46 ages between 0.1 and 18 Gyr. The lack of younger ages is due to the lack of hot stars in MILES.

3.4 Galaxev and MILES/GRANADA

Charlot & Bruzual (2009 in prep.) have produced models analogous to those in BC03, but replacing STELIB by a combination of the MILES and GRANADA libraries. The latter are used only for hot stars. These models, kindly provided by the authors in advance of publication, are still preliminary. The models used here have a Chabrier IMF and Padova 1994 tracks, with the same 221 ages and 6 metallicities in BC03.

3.5 Summary of the set of models

Table 2 summarizes the basic properties of the different sets of SSP models used in this work. There are 7 sets of models, differing in at least one of the following: evolutionary synthesis code (Galaxev, SED@, and Vazdekis), stellar tracks (Padova 1994 and 2000), IMF (Chabrier, Salpeter) and stellar library (STELIB, MILES, GRANADA). Independent combinations of these four ingredients would produce a grid of $3 \times 2 \times 3 \times 3 = 54$ model-sets, but this is not how one finds these models in their respective web repositories. Furthermore, the sets of metallicities are not identical among all models, and there are also differences in the ages for which SSP spectra are tabulated. Comparisons of results achieved with different models must take into account this non-uniformity, which is an example of one of the difficulties faced by model users.

The spectral fitting methodology described in Paper I was applied to all 27 SC spectra. As explained there, the fits are carried out feeding STARLIGHT with a single Z base containing all N_t ages in a model, and then repeating things for other Z's. The $N_Z = 6$ V00s bases in Paper I expand to 39 bases to account for all models in Table 2. Note that while the sampling in age is practically continuous, predictions are only available for 6 metallicities (3 in the case of the GRANADA models), an apparent "technicality" which has

a non-negligible impact in our analysis, and is not fully cured by interpolations (see Paper I).

3.6 Notation

Throughout this paper these models will be referred to using the codes given in Table 2. Alternatively, we will refer to BC as the STELIB models, CB and V as the MILES models, and RG as the GRANADA models. For convenience, metallicities will be transformed to a log-solar scale. In this notation, the Z values 0.05, 0.03, 0.019, 0.008, 0.004, 0.001, 0.0004 and 0.0001 covered by the models correspond to (rounding up to the first decimal) $\log Z/Z_\odot = +0.4, +0.2, 0, -0.4, -0.7, -1.3, -1.7$ and -2.3, respectively. (Notice that we do not distinguish between $Z = 0.019$ and 0.020). This will be applied both to the metallicities from the stellar tracks and [Fe/H] from the literature. Ages will be given in yr throughout.

4 RESULTS: QUALITY OF THE SPECTRAL FITS

As a first step in the exploration of our results, this section investigates the quality of the spectral fits obtained with different models. Given the size of the data set (27 SCs $\times$ 7 models), we concentrate this comparison on results for a couple of illustrative examples (the same used in Paper I), which also help clarifying several of the issues discussed in the next sections.

Fig. 1 shows the spectral fits to the LMC cluster NGC 2010. To first order all fits (right panels) are of similar quality, as can be appreciated by the similarity of the residual spectra plotted (multiplied by 3 for clarity). The mean percentage deviations ($\overline{\Delta}$) vary from 1.8 (RG00s) to 2.4% (BC00s), a relatively narrow range which shows that, at least in the case of this young metal rich SC, it is hard to distinguish models on the basis of fit quality alone.

As discussed in Paper I, our χ^2 values are not in a meaningful absolute scale, but can be used to rank the fits. In analogy with the index defined in Paper I to compare fits of different t, Z, and A_V but same model set, we will use

$$\delta = \frac{\chi^2 - \chi^2_{best}}{\chi^2_{best}} \quad (1)$$

to compare fits obtained with different models, with $\delta = 0$ denoting the best one (RG00s in the case of NGC 2010).

Values of δ are listed in Fig. 1, along with the resulting model ranking (numbers within brackets). The δ values for
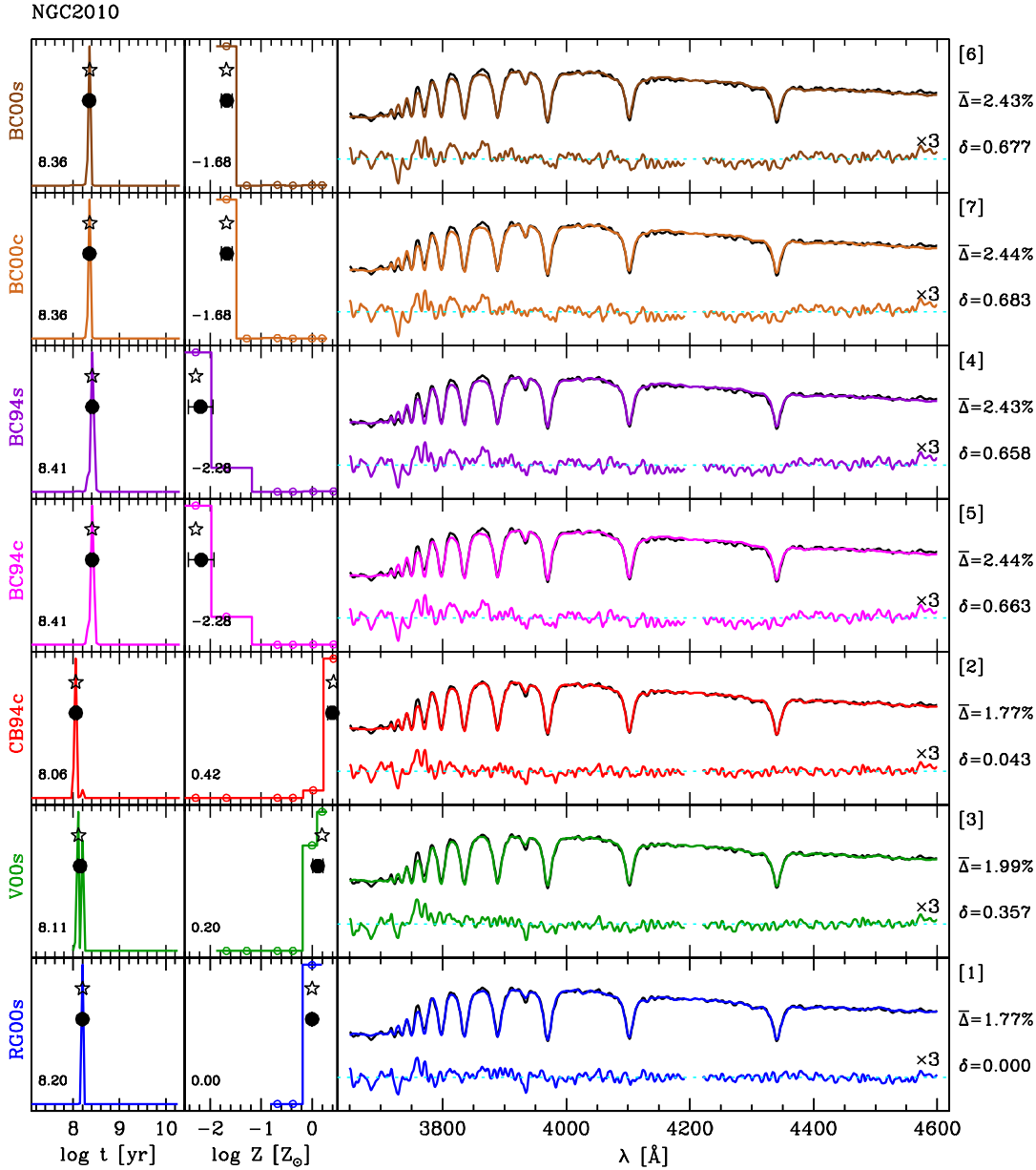
Figure 1. Comparison of spectral fits of NGC 2010 obtained with 7 different evolutionary synthesis, labeled in the left axis (see Table 2). Right panels show the observed (O_λ, in black), best fit (M_λ, colored), and $R_\lambda = O_\lambda - M_\lambda$ residual spectra. All spectra are normalized at 4020 Å, and the dashed line marks the zero flux level. *Notice that R_λ is multiplied by 3 for clarity.* Values of the mean percentage residual ($\overline{\Delta}$) are listed to the right of each panel, where the number in brackets indicate the χ^2 fit quality ranking, and $\delta = (\chi^2 - \chi^2_{best})/\chi^2_{best}$. The left panels show the probability distribution functions of t and Z. A solid circle with error bars marks the mean ± 1 sigma estimates. The numbers correspond to the best fit t (left most panel) and Z (middle), whose values are also marked by a star. In the middle panel, open circles are plotted in each of the metallicities in the base.

NGC 2010 show that RG00s and CB94c models are nearly equally good, with the V00s models coming in third place. The STELIB based models not only produce the worse spectral fits, but their t and Z values differ a lot from the others, as can be seen in the probability distribution functions (PDF) plotted on the left and middle panels.

Moving to the other end of the t-Z space, results for the old and metal poor cluster NGC 2210 are shown in Fig. 2. In this case the CB94c and V00s models are visibly much better than the others. This is reflected by the δ values, which are > 2 for all other models (indicating fits over 3 times as worse in terms of χ^2). The RG00s models, which performed so well for NGC 2010, are by far the worst in this case. The reason for this is that the RG00s models start at
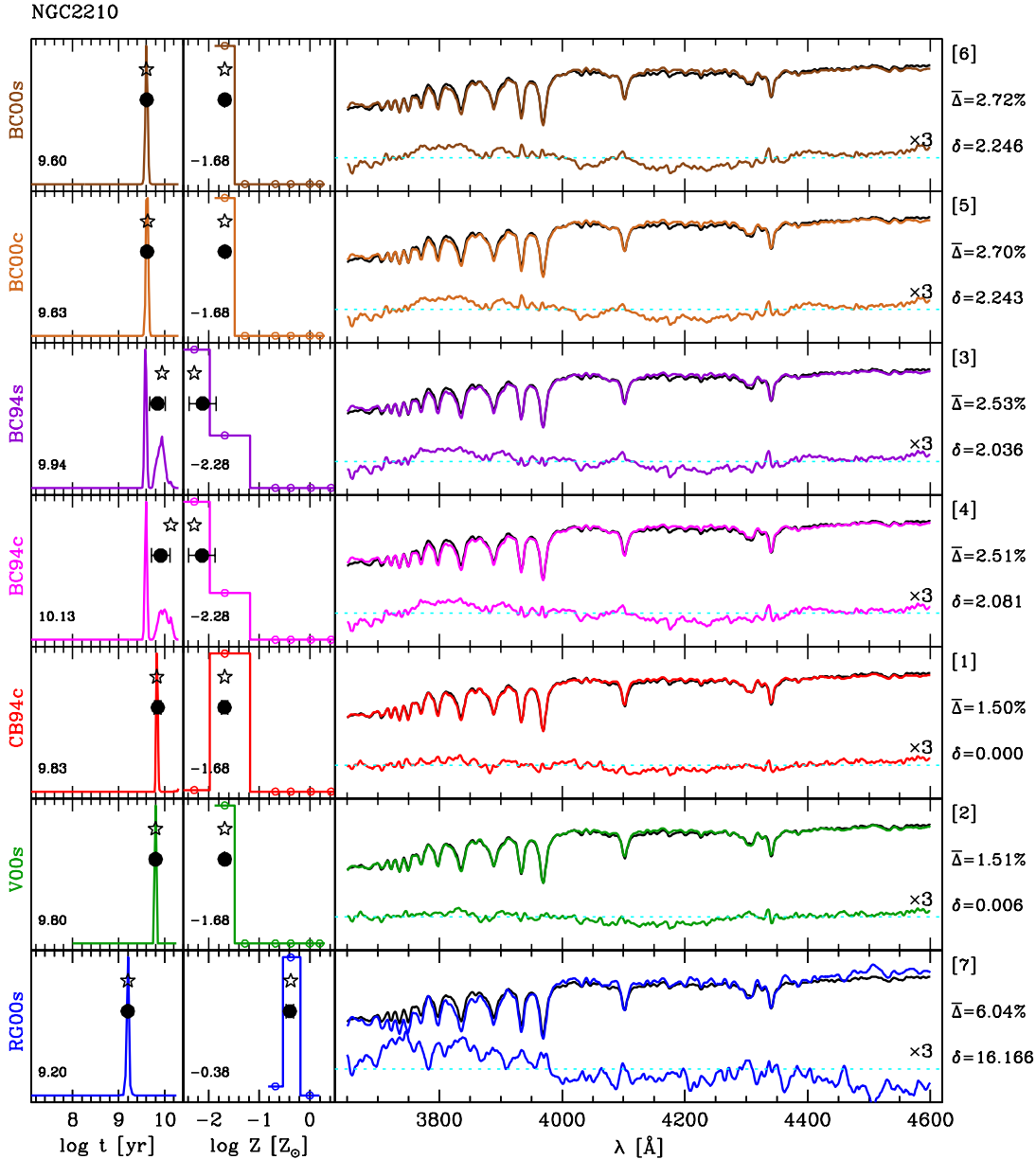
Figure 2. As Fig. 1, but for NGC 2210

log $Z/Z_\odot = -0.7$ which is much larger that the metallicity of this SC (Table 1). This also happens for NGC 416, NGC 1754, M15 and M79. Besides, it is well known that theoretical libraries perform better for hot than for cool stars (e.g. Martins & Coelho 2007; Bertone et al. 2008), so one expects the GRANADA models to work better for young than for old SCs, irrespective of their metallicity. This is confirmed by the case of 47 Tuc. With log $Z/Z_\odot = -0.76$ (Table 1), this SC is not too far off the lower Z limit of the GRANADA models, but because of its old age (log $t = 10.1$), the RG00s models provide the worse spectral fits (Tables 3–8).

These examples suggest that, at least in some cases,

spectral fitting can, by itself, help distinguish among competing models. Another conclusion of this preliminary analysis is that models based on the MILES library tend to produce better spectral fits than those based on STELIB. The same can be said about the GRANADA models if one concentrates on young and intermediate age SCs. This is rewarding in the sense that it shows that more recent libraries (MILES and GRANADA) do represent an improvement upon older ones (STELIB), at least insofar as spectral fit quality is concerned and as long as the limitations of the models are not overlooked.

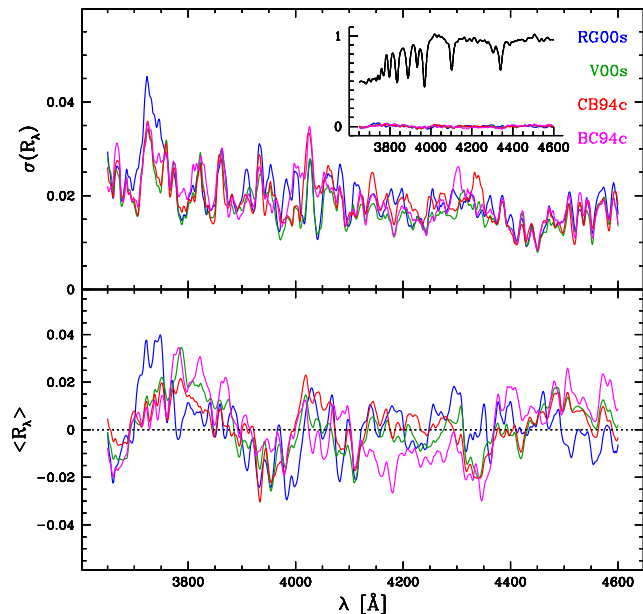On the whole, however, these improvements are rela-

Figure 3. Mean (bottom) and standard deviation (top) of the spectral residuals for the 13 SCs in the sample whose ages and metallicities are within the ranges spanned by all models: NGC 1651, NGC 1783, NGC 1806, NGC 1831, NGC 1846, NGC 1978, NGC 2010, NGC 2133, NGC 2134, NGC 2136, NGC 2203, NGC 2213 and NGC 2249. The inset shows the same residuals as in the bottom panel, but plotted on the scale of the mean observed spectrum (black line). All spectra have been smoothed by 10 Å boxcar for clarity.

tively subtle, only marginally captured by global fit quality measures. For instance, restricting to 13 SCs whose t and Z literature values fall within the nominal range of validity of all models considered here, we find sample mean values of $\overline{\Delta} = 2.15$, 2.19 and 2.38% for V00s, CB94c and RG00s models, respectively, while for the STELIB models the values range from 2.42 to 2.51%. These small differences are further illustrated in Fig. 3, where we plot the mean residual spectrum (bottom) and its standard deviation (top) for the same subset of 13 SCs. For clarity, all spectra have been smoothed by 10 Å. Because of its vertical scale, the plot may convey the wrong impression that residuals are large. To show that this is not the case, the inset shows the same mean residuals as in the bottom panel, but plotted on the more relevant scale of the mean spectrum.

The general message from Fig. 3 and the sample mean $\overline{\Delta}$ values quote above is the same. They both confirm that progress is being made, but they also show that, from the point of view of fit quality, these are small improvements upon models which were already good. This highlights the need to extend these tests from the space of observables (spectra) to that of derived properties (t, Z and A_V). That is the subject of the next sections.

5 RESULTS: COMPARISON OF PROPERTIES DERIVED WITH DIFFERENT MODELS

We now turn to a comparison of the SC properties derived from spectral fits with different models. Our goal here is to evaluate the dispersion and systematic differences in t, Z and A_V stemming from the use of different ingredients in the spectral analysis.

For each of t, Z, and A_V, the methodology outlined in Paper I provides two estimates: The best fit value and the mean value obtained from the full PDF; subscripts 'best' and 'PDF' are used to distinguish them when necessary. Both estimates are shown in the PDF panels in Figs. 1 and 2, where stars mark $t_{\rm best}$ and $Z_{\rm best}$ and solid circles with an error bar show the PDF based estimates.

Tables 3–8 give these estimates for all SCs and 6 of the 7 models considered here except for V00s, whose results were already presented in Table 1 of Paper I. Other entries in these tables give the mean percentage deviation ($\overline{\Delta}$) of the best fit model and quantities related to the multi-SSP fits (see Paper I for details). From the discussion in Paper I (see also Koleva et al. 2008), in a few cases (NGC 2210, M15, M79) multi-SSP fits detect the presence of a hot and old population not well accounted for by single SSP models, indicating the presence of a blue Horizontal Branch (HB). In such cases, the age of the oldest component (column 10 in Tables 3–8) is arguably a better age estimate than either $t_{\rm best}$ or $t_{\rm PDF}$. In the case of NGC 2210 and for the V00s models, for instance, this third estimate gives an age ~ 0.3 dex older than that found with single-SSP fits, and in better agreement with the literature data.

We concentrate our analysis on the PDF-based (or "bayesian") estimates of t, Z and A_V. Barring caveats like systematic effects associated to SCs with blue HB's, we consider these our more consistent estimates of SC properties.

Figs. 4, 5 and 6 plot $t_{\rm PDF}$, $Z_{\rm PDF}$ and $A_{V,\rm PDF}$ for all models and SCs in the sample. Each SC is identified by an ID number (see Table 1), and each set of models is coded by a color. One should note that formal parameter uncertainties (the PDF-based standard deviations, plotted as error bars) are themselves subjected to uncertainties and biases due to model limitations. The fact that the GRANADA models (blue points) do not extend to metallicities as small as that of many of our SCs leads to underestimated $\sigma(\log Z/Z_\odot)$ values. Similarly, because of the lack of $t < 10^8$ yr models in the Vazdekis grid, the derived $\sigma(\log t)$ values are too small for the youngest SCs. In any case, even taking these caveats into consideration, these plots show that formal statistical uncertainties are smaller than the differences stemming from use of different models. In what follows we quantify and discuss the reasons for these differences.

5.1 Ages

Fig. 4 shows, for each SC, the bayesian age obtained with each of the seven models. For most objects, the formal uncertainty in $\log t$ is small, indicating that the fit is well constrained around a given combination of t and Z in the base models.

To provide a visual sense of the significance of our PDF-based uncertainties in age, Fig. 7 shows CB94c models for NGC 2210 for 5 ages: the PDF estimate $\log t = 9.86$ (dotted
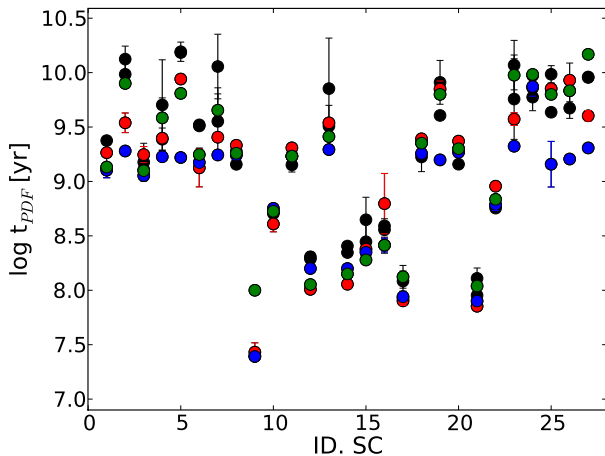
Figure 4. Age estimates obtained from the spectral fits of each cluster for each set of evolutionary synthesis models, coded by color: STELIB models (only BC00s and BC94c) results are plotted in black, CB94c models in red, RG00s models in blue, and V00s models in green circles. Every point has an error bar, but only the STELIB (black) ones stand out clearly.
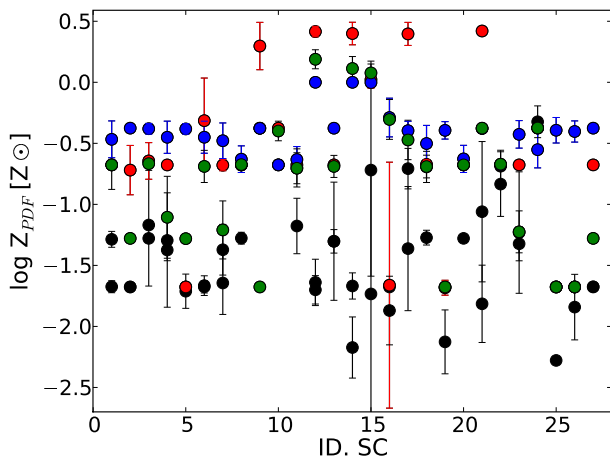

Figure 5. As Fig. 4, but for the metallicity.

Figure 6. As Fig. 4, but for the extinction.
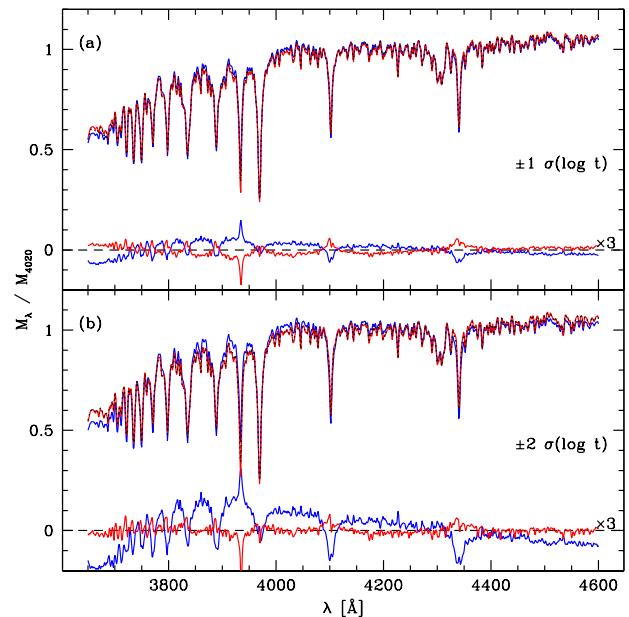
Figure 7. Comparison of CB94c models of different ages for NGC2210. Dotted lines show the model whose age is the closest to our PDF-based estimate ($\log t = 9.86$). Blue and red lines in panel (a) show the models at ages one $\sigma(\log t)$ above and below $\log t_{\mathrm{PDF}}$, while in (b) models with ages $\pm 2\sigma(\log t)$ from $\log t_{\mathrm{PDF}}$ are plotted. Models are shown at their original spectral resolution, and residuals are multiplied by 3 for clarity. The plot illustrates the sort of spectral differences expected for parameters within 1 and 2 sigma of their estimated values.

lines), plus models with ages one (top) and two (bottom) sigmas away from this value. Since $\sigma(\log t) = 0.09$ (Table 3), the models shown span the $9.68 < \log t < 10.04$ interval. All SSP spectra correspond to $\log Z/Z_\odot = -1.7$, but A_V varies from 0.26 (at $\log t_{\mathrm{PDF}} - 2\sigma$) to 0.12 (at $\log t_{\mathrm{PDF}} + 2\sigma$), in a way to always produce the best possible match to the observed spectrum. The plot shows that models are indeed spectroscopically different even at a $\pm 1\sigma(\log t)$ level, which gives qualitative support to our formal error estimates. It is nevertheless necessary to point out that in many cases the quality of the fit deteriorates so quickly even for adjacent ages in the grid that $\sigma(\log t)$ becomes < 0.01, in which case no uncertainty is quoted (these are the ± 0.00 entries in Tables 3–8). This happens often in the V00s models, as a result of their relatively coarse (0.05 dex) sampling in age. As pointed out in Paper I, in such cases it is more advisable

to take half of the grid sampling as a more realistic (albeit less formal) estimate of $\sigma(\log t)$.

In some cases, however, $\sigma(\log t)$ is relatively large. The broadest age PDFs (larger uncertainty in t) are found with STELIB models (see Fig. 8). The example of NGC 2210, whose t and Z PDFs are shown in Fig. 2, illustrates that such large values for $\sigma(\log t)$ stem from the inability to distinguish among different Z's. The PDF(Z) for the BC94 fits is broad,

covering the 2 smallest values in the grid ($\log Z/Z_\odot = -2.3$ and -1.7). To each of these two acceptable Z's there is a corresponding peak in PDF(t), producing a large $\sigma(\log t)$[8]. This ambiguity arises from the fact that STELIB contains very few truly low Z stars, so the predicted SSP spectra for these two Z's use essentially the same stars, differing only in their proportions (dictated by the evolutionary tracks). This leads to similar predicted SSP spectra, explaining the inability of spectral fits to distinguish the two solutions. In other words, there is a severe mismatch between the metallicities of the stars in the library and the nominal Z of the models, which is that corresponding to the evolutionary tracks. This caveat is acknowledged and discussed by BC03, who classify their two lowest metallicity models as "poor" for < 1 Gyr populations and "fair" for older ones (compare this to the "very good" mark ascribed to $Z_\odot$ models of any age).

A similar conclusion arises when $t_{\rm PDF}$ is plotted against $t_{\rm best}$. Naturally, these two quantities correlate strongly, but the few points out of the correlation correspond to STELIB fits, and these outliers are also points that have the largest $\sigma(\log t)$. Thus, ages are more poorly constrained with the STELIB models.

Notwithstanding these caveats, the age estimates obtained with all models are fairly consistent with each other. This is illustrated in Fig. 9, where we plot the bayesian ages of RG00s, V00s and BC models against those obtained with the CB94c models.

The largest discrepancies seen in Figs. 4 and 9 are associated to fits of SCs whose ages or metallicities fall outside the range of validity of the models, causing expected biases. NGC 1818 (ID. 9 in Fig. 4), for instance, has a CMD age of 20 Myr (Table 1). All the models, except V00s, give an age in agreement with the CMD age. The reason why the V00s models fail for this SC is simply that their youngest age is 100 Myr, which is in fact the best fitting age found by STARLIGHT (for lack of a better alternative). NGC 1754 (ID. 5 in Fig. 4) is another example. Most of the models obtain an age which is similar to the CMD value ($\log t = 10.2$), but the GRANADA models yield an age of $\log t = 9.2$, a factor of 10 too low. This failure occurs because the lowest metallicity available in the RG00s models is $\log Z/Z_\odot = -0.7$, much higher than the metallicity of NGC 1754 ($\log Z/Z_\odot = -1.4$, according to Table 1). Due to the age-metallicity degeneracy, forcing a larger Z results in an underestimated t. A similar effect is seen in Fig. 2, where the RG00s models produce the smallest ages.

In short, the RG00s models are simply not applicable to metal poor SCs, and the V00s cannot be applied to systems younger than 100 Myr. Except for such violations of the range of validity, all models provide reasonably consistent age estimates.

Because our sample is composed of well studied objects, with plenty of t and Z estimates in the literature, it is straightforward to identify such violations. Obviously, such information is not generally available for other systems, and in fact this is precisely what one aims to derive through spectral synthesis. It is therefore useful to show results obtained

Figure 8. Distributions of $\sigma(\log t)$ and $\sigma(\log Z/Z_\odot)$ versus the set of models used in the fits. Each point represents the result obtained for each cluster and each set of models. The error bars represents the mean and the standard deviation of the distribution for each set of models. Points and error bars plotted in red correspond to the subset of 13 clusters which fall within the range of validity of all models considered here (the same ones listed in Fig. 3).

stretching models beyond their nominal range of validity, as done above. This "deliberate mistake" produces illustrative examples of the sort of spurious results that one would obtain in practical work, where the same mistake can be made unadvertedly.

5.2 Metallicity

Fig. 5 shows the metallicities obtained for each cluster with the seven sets of models. In contrast with the age results, the dispersion in the metallicity is significant, in most cases much larger than the error bars.

One source for this large dispersion is the already mentioned violation of the limits of the RG00s and V00s models. As expected, metal poor SCs (IDs 2, 5, 12, 21, 25, and 26 in 5, which have $\log Z/Z_\odot \leqslant -1.2$) are badly fitted with the GRANADA models, which are valid only for $\log Z/Z_\odot \geqslant -0.7$. This also explains why the Z values for the RG00s fits cover such a narrow range (see also Fig. 10). Also, the V00s value of the metallicity of NGC 1818 is severely un-

---

[8] The BC00 models would most likely exhibit the same behavior if their Z's reached values as low as in BC94 (the lowest $\log Z/Z_\odot$ in the BC00 models is -1.7).
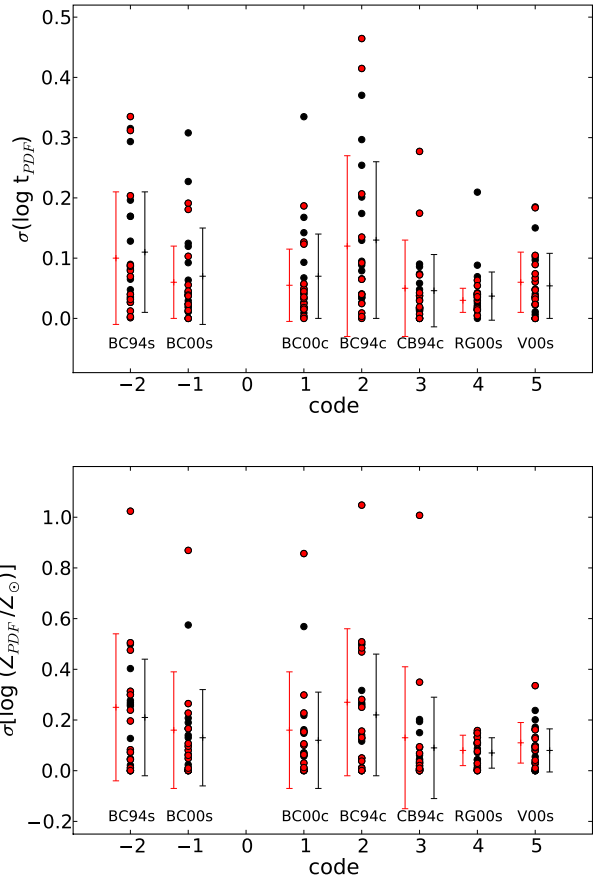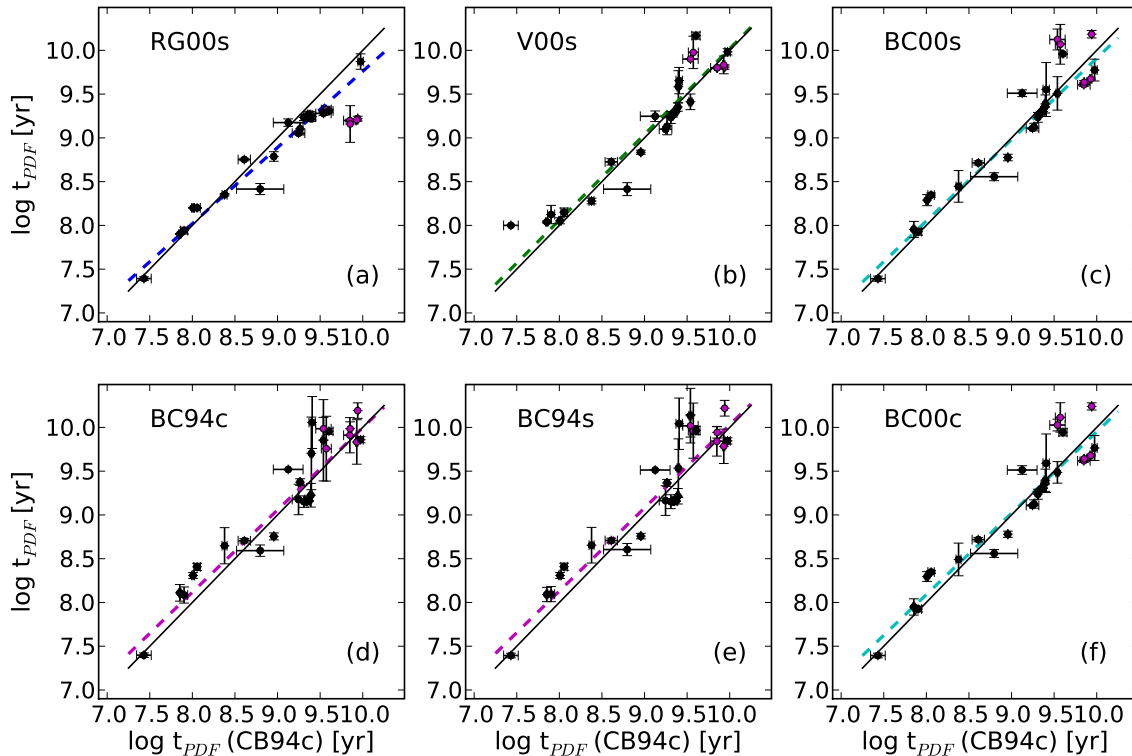
Figure 9. Correlation between the bayesian ages obtained for each set of models as a function of the ages obtained with CB94c models. The black line is the one-to-one relation, and the dashed line shows a linear fit.

derestimated to compensate for its overestimated age of 100 Myr, the youngest SSP in these models.

Even disconsidering these cases, the dispersion in Z values remains large. As evident to the eye in Fig. 5, much of this dispersion is caused by the STELIB results, which in most cases produce Z values well below those obtained with other models. Most of the STELIB results are below 0.1 solar, and none are solar or above. As seen in Fig. 10, the STELIB metallicity distribution peaks at $\log Z/Z_\odot = -1.6$, while other models peak around -0.7. Besides this bias, STELIB models also lead to larger formal uncertainties in Z, as shown in Fig. 8. The reason for this is the already discussed similarity of SSP spectra for the lowest Z's in BC03. These results remain valid restricting the analysis to 13 SCs whose t and Z literature values fall within the nominal range of validity of all models considered here (the red points in Fig. 10 correspond to the SCs in Fig. 3).

It is important to point out that although throughout this paper we group the BC94 and BC00 models as "STELIB models", there is an important, albeit apparently technical, difference between them: The BC94 models have a coarser but wider Z-grid, extending down to $\log Z/Z_\odot = -1.7$ and -2.3, whereas the BC00 models stop at -1.7. The similarity between the $\log Z/Z_\odot = -1.7$ and -2.3 spectra in the BC94 models leads to larger t and Z uncertainties than obtained with the BC00 models, as can be seen in Figs. 8 and 10. Had we ignored the $\log Z/Z_\odot = -2.3$ BC94 models, these differences in $\sigma(\log t)$ and $\sigma(\log Z/Z_\odot)$ would be smaller,
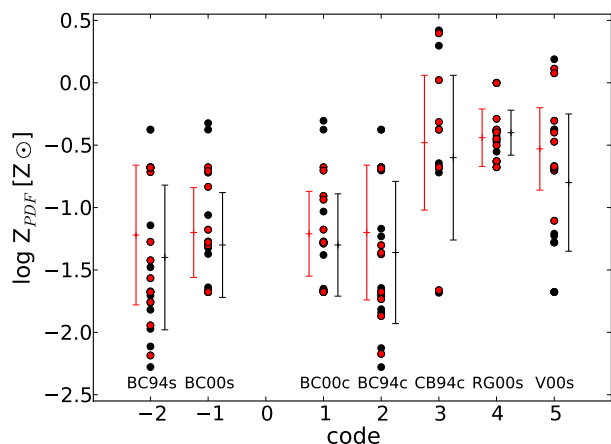

Figure 10. Distribution of the metallicity ($\log Z/Z_\odot$) versus the set of models (code) used. The error bars represent the mean and the standard deviation of the $\log (Z/Z_\odot)$ distribution for each set of models considering the whole sample of clusters (black) and only 13 clusters in Figure 3 (red).

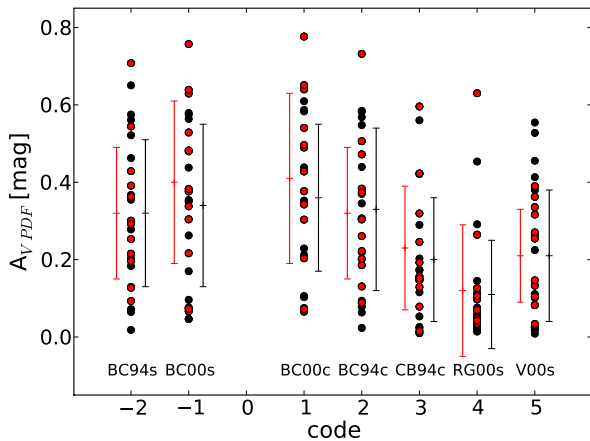but still larger than those obtained with GRANADA and MILES models.

Figure 11. As Fig. 10, but for the V-band extinction, A_V.

5.3 Extinction

Fig. 6 shows for each SC the bayesian extinction obtained with each set of models. The values obtained range from 0 to 0.8, with significant model to model differences. As it happens with Z, the STELIB results for A_V differ systematically from those derived with the MILES and GRANADA models, as better seen in Fig. 11. The average extinction with STELIB, MILES and GRANADA libraries is 0.34, 0.20, and 0.11, respectively. The uncertainty in A_V is also larger with STELIB, which produces an average $\sigma(A_V)$ of 0.1, whereas for other models the average $\sigma(A_V)$ is 0.06.

6 RESULTS: SPECTRAL FITTING RESULTS VS. DATA IN THE LITERATURE

Despite their relevance, the internal comparisons performed in section 4 cannot, by definition, provide an absolute measure of the adequacy of the results achieved with different models. This section presents this most critical test. We compare the ages, metallicities and extinctions derived from spectral fits with those reported in the literature. We also discuss the capabilities and limitations of each of seven sets of evolutionary synthesis models to reproduce the results from S-CMD work or with Rose's indices.

6.1 Ages

Fig. 12 compares our PDF based ages with the S-CMD ages compiled by LR03, listed in Table 1. Each panel shows results obtained for one of the seven sets of models in Table 2. In all cases the correlation is very good. Two linear fits are presented in each panel: Dashed lines show the fits obtained using all 27 SCs, while the solid lines represent fits excluding the five SCs with $\log Z/Z_\odot \leqslant -1.2$ (NGC 416, NGC 1754, NGC 2210, M15 and M79). The latter fits filter out the difficulties faced by some models at low metallicities, like the absence of GRANADA models for $\log Z/Z_\odot < -0.7$ and the lack of very metal poor stars in STELIB (see section 5). On the other hand, these SCs allow us to test the capability of the models to estimate correct ages even when Z is a factor of three lower than in the models.
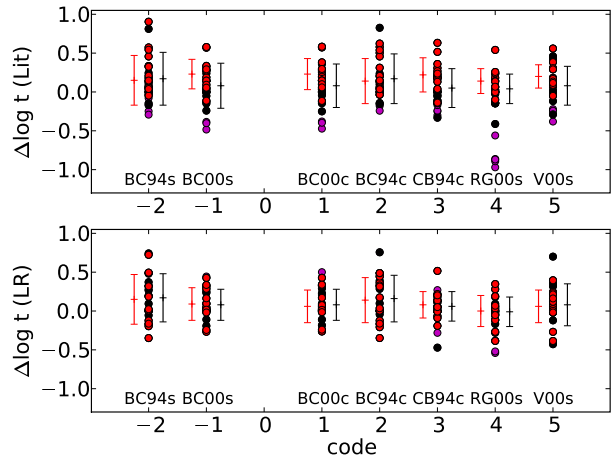
Figure 13. Logarithmic difference between the spectral fit age obtained for each set of models and the literature age tabulated in Table 1. Magenta circles mark the metal poor clusters ($\log Z/Z_\odot \leqslant -1.2$). In the top panel STARLIGHT ages are compared to S-CMD ages, while in the bottom panel the STARLIGHT ages are compared to the LR03 estimates. Error bars mark the mean and standard deviation for each set of models considering the whole sample (in black) and only the 13 clusters in Fig. 3 (red).

A general conclusion from Fig. 12 that our spectral fitting ages are slightly older than the S-CMD ages. Most of the points and linear fits are located above the identity line. Only the GRANADA linear fit, when all the SCs are included, crosses this line, and exclusively due to the effect of the most metal poor SCs, whose ages come out severely underestimated due to the lack of SED@ models for $Z < 0.2$ solar. Because stellar evolution runs faster at higher metallicities, the ages predicted for these metal poor SCs are much younger if models with isochrones of higher metallicity are used. In the other sets of models, the ages of these SCs are relatively well predicted because they include tracks that follow stellar evolution at metallicities below 0.2 solar ($\log Z/Z_\odot = -1.3$, -1.7 and -2.3). This conclusion also holds for the BC fits, despite the incompleteness of the STELIB library at low Z.

This suggests that the capability of the models to match the ages of metal poor clusters is driven more by the evolutionary tracks than by the stellar spectral library. This was pointed out before by González Delgado et al. (1999), who were able to match the ages of LMC clusters fitting the high order Balmer lines using models with an empirical library of $Z_\odot$ stars but following the evolution with tracks at low Z. The explanation is simple. The strength and shape of the Balmer absorption lines depend on the effective temperature and gravity, but not on Z. The spectral range that we are fitting is dominated by the Balmer lines and the Balmer jump, which mainly depend on effective temperature of the main sequence turn off. Thus, the ages predicted for metal poor clusters that are fitted by models for which the evolution is described by stellar tracks at higher metallicity will be smaller than the real age. As long as the tracks cover the correct metallicity range, ages come out in good agreement with CMD data, regardless of the library.

Figure 12. Panels a, b,c, e and f: Correlation between the age obtained with STARLIGHT and the ages in Table 1 derived with the S-CMD calibration. Each panel represents the result for each set of models as labelled in the upper left corner. Metal poor clusters ($\log Z/Z_\odot \leqslant -1.2$) are marked with magenta circles. The black line is the one-to-one relationship, the dashed line is the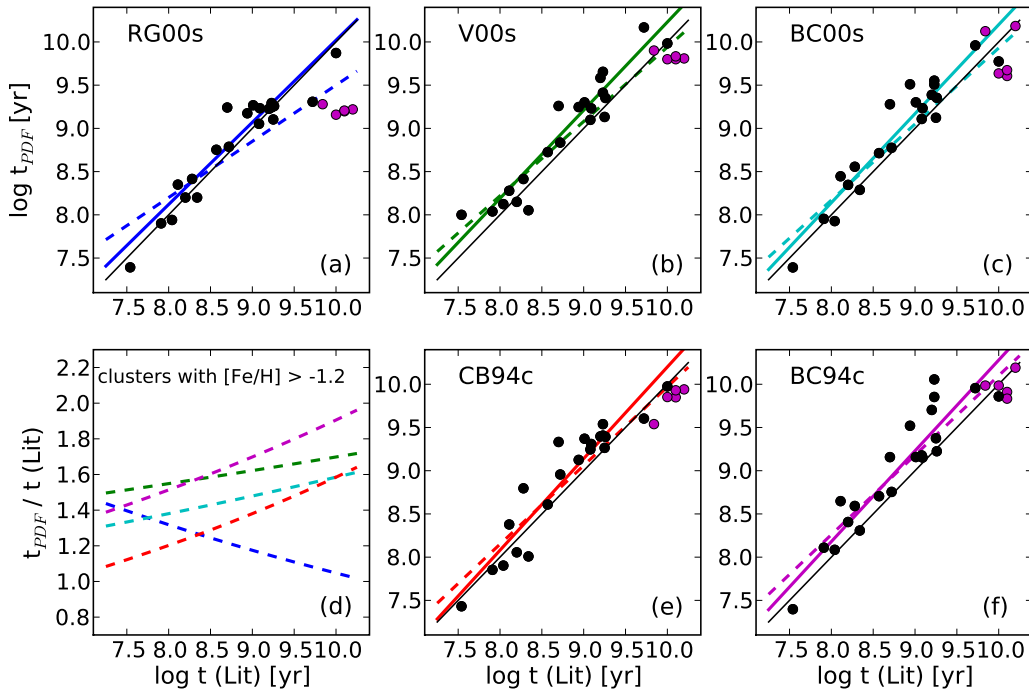 result of the linear fit to all the points, and the solid line the result of the linear fit excluding the metal poor clusters. The bottom left panel shows the deviation of the linear fit obtained for each set of models with respect to the one-to-one relationship, expressed as the ratio between the spectral fit and literature ages.

Fig. 13 summarizes the comparison of ages. It shows the distributions of $\Delta \log t = \log t_{PDF} - \log t_{Lit}$ for different models. Red circles mark the 13 SCs within the nominal range of validity of all models studied here. In the top panel the literature age t_{Lit} is that from S-CMD estimates, while in the bottom one the age obtained from Rose's spectral indices (LR03) is used. Magenta circles mark the five metal poorest SCs. Neglecting these objects and using only the S-CMD ages, the mean values and sample standard deviation of $\Delta \log t$ are 0.04 ± 0.20 for the RG00s models, 0.12 ± 0.23 for CB94c, 0.17 ± 0.21 for V00s, and from 0.14 ± 0.22 to 0.23 ± 0.29 dex for the STELIB ones. Somewhat smaller differences are obtained using the LR03 age estimates: -0.01 ± 0.19 (RG00s), 0.06 ± 0.19 (CB94c), 0.08 ± 0.27 (V00s), and from 0.08 ± 0.20 to 0.17 ± 0.30 dex (BC models). These statistics are represented as error bars in Fig. 13.

In summary, the main conclusions of this section are:

(i) Spectral fits with STARLIGHT provide ages that are within a factor better than 2 of the S-CMD ages.

(ii) The spectral fit ages are more similar to the Rose's age estimations than to S-CMD ages.

(iii) Fits with models based on the GRANADA and/or MILES libraries can date young and intermediate stellar clusters better than the models with the STELIB library.

(iv) However, the age of metal poor SCs is not well constrained if the models do not include evolutionary tracks at the correct metallicity range. Thus, at low Z, the evolutionary tracks is the main ingredient in the models to predict the age of young clusters.

6.2 Metallicities

In contrast with the age results, the correlation between the STARLIGHT metallicities and literature values (from the CaII triplet or the Rose's indices; see values in Table 1) is poor. This result was expected considering that $\sigma(\log Z/Z_\odot)$ is typically two times larger than $\sigma(\log t)$, and that Z covers a 1 dex smaller dynamic range than t. This is also a consequence of the discrete metallicity grids, with a maximum of only $N_Z = 6$ Z values in any given model, covering a wide range from $1/200$ to 2.5 solar. Because the step in Z in each set of models is at least of a factor 2, we consider that the Z is well estimated if the difference between the STARLIGHT metallicity and the literature values is $\leqslant$ a factor 2.[9]

As done for the ages, we define $\Delta \log Z/Z_\odot$ =

---

[9] As discussed in Paper I, interpolating grids in Z alleviates somewhat the discreteness effects, but the errors in the interpolated spectra are of the same order of the spectral residuals obtained in the actual data fits, such that the overall gain in resorting to interpolated grids is not significant. Experiments with the V00s models also show that the Z-estimates obtained with Z-interpolated grids do not lead to a better agreement with the literature values.
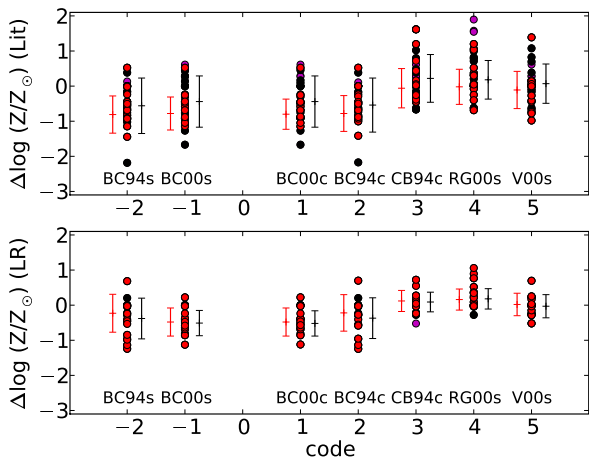
Figure 14. As Fig. 13 but for metallicity. At the top panel, the STARLIGHT Z are compared to CaII triplet metallicities from Olszewski et al. (1991), while in the bottom panel the comparison is made with respect to the estimates made by LR03.

$(\log Z/Z_\odot)_{\rm PDF} - (\log Z/Z_\odot)_{\rm Lit}$ as the logarithmic difference between our Z values and those in the literature. $Z_{\rm Lit}$ can be based either on the CaII triplet or Rose indices (LR03; see Table 1). These two literature estimates differ typically by 0.18 dex, with $Z_{\rm LR03}$ smaller than $Z_{\rm CaT}$. This gives a measure of how consistent these estimates are. Naturally, this dispersion on our reference values propagates to $\Delta \log Z/Z_\odot$.

Fig. 14 shows the results obtained for each set of models, in the same format as Fig. 13. The results that come out from these plots are:

(i) On average the CaII triplet metallicity differs from our $Z_{\rm PDF}$ by a factor of 4.

(ii) Excluding metal poor SCs, only 10% of the STELIB fits have metallicities that differ by less than a factor 2 with respect to the CaII triplet metallicity, but in ∼40% of the MILES or GRANADA fits the difference is less than a factor 2.

(iii) STELIB provides metallicities that are significantly underestimated with respect to both the CaII triplet and LR03 metallicities. A similar conclusion was derived by Koleva et al. (2008) in their analysis of Galactic globular clusters.

(iv) On average, the Vazdekis models estimate metallicities that agree better with the CaII triplet metallicity than the estimations with other models.

6.3 Extinction

The extinction data for each cluster that are available in the literature and listed in Table 1 are very disperse. This can be seen, for instance, by the lack of correlation between the extinction derived from the MCPS, the CMD, and McLaughlin & van der Marel (2005). These three sets of literature values lead to average A_V values of 0.41, 0.25 and 0.06, respectively. Our spectral fits results are in between them, leading to average extinctions of 0.32, 0.20 and 0.11 for STELIB, MILES and GRANADA models, respectively. This is as much as

can be said about A_V estimates, as the inhomogeneity of the literature data prevents a more detailed comparison.

7 DISCUSSION

7.1 Caveats: Stochastic fluctuation effects

Evolutionary synthesis models always assume that the cluster is massive enough such that all stages are well sampled, and by applying these models we have subscribed to this hypothesis. When a cluster is not very populated, stochastic fluctuations may play an important role in the determination of its properties. Studies dedicated to this issue have shown that stochastic effects can easily dominate the integrated light, and that the impact varies with wavelength and age (e.g. Cerviño et al. 2000; Cerviño & Luridiana 2004, 2006; Lançon & Mouchine 2000). This raises the question of whether we are entitled to neglect such effects in our analysis.

A way to answer this question is to compared the SC luminosity at a given wavelength with the contribution of the brightest star in this band. We have compiled from the literature the V magnitude of the MC clusters of the sample. V ranges from 9.8 to 12.4, with a mean absolute magnitude of $M_V = -7.2$ or $\log L_V = 34.5$ (erg s^{-1} Å^{-1}). The younger SCs of the sample are more luminous than the mean, and the weakest ones are those with an intermediate age, 1–2 Gyr.

Following Cerviño & Luridiana (2004) and using the GRANADA models, we have obtained the minimum luminosity of a SC that ensures that the fluctuations are less than 10% of the mean luminosity ($L_{10\%}$). We have also obtained the lowest luminosity limit (L_{LLL}), which requires the total luminosity of a cluster to be larger than the contribution of the brightest star included in the isochrones. If the luminosity of the cluster is larger than $L_{10\%}$ and L_{LLL}, then stochastic effects may be safely neglected.

In the V band, these two quantities are $\log L_{10\%} = 34.2$, 33.7, 33.4, and $\log L_{LLL} = 33.4$, 32.7, 32.4 (erg s^{-1} Å^{-1}), for ages of 0.2 , 2 and 10 Gyr, respectively. These values are well below the average V band luminosity of our SCs. Considering that stochastic fluctuations are even less important in the B and U bands (the spectral range covered by the spectra analyzed here), we can conclude that these effects are not important for these clusters. This is true even for the weakest objects with $\log L_V = 34.0$ (erg s^{-1} Å^{-1}) because they are about 1–2 Gyr old, when the stochastic fluctuations have a very small impact at the B and U bands (cf. Figs. 1 and 3 in Cerviño & Luridiana 2004).

7.2 Caveats: The abundance ratios

Another issue that deserves discussion is the inconsistency between the chemical abundance pattern of the models and data. In massive elliptical galaxies, the mismatch between their "α-enhanced" stellar populations (Worthey, Faber & Gonzalez 1992) and evolutionary synthesis models which do not take this into account lead to clearly identifiable residuals in spectral fits (e.g., Panter et al. 2007). Are analogous effects present in our SCs, and if so, how does this affect our analysis?

The stellar spectra of the GRANADA models were computed with solar scaled abundances for all metallicities, while the Galaxev and Vazdekis models are based on empirical libraries built from nearby stars, and thus track the relation between $[\alpha/Fe]$ and $[Fe/H]$ of the solar neighborhood, where $[\alpha/Fe]$ grows from 0 at $Z_\odot$ to $\sim +0.4$ dex at low metallicity (below $[Fe/H] = -0.7$; McWilliam et al. 1994). Field stars in the LMC follow a different pattern (Pompéia et al. 2008 and references therein). Some α-elements like Ca, Si, and Ti show X/Fe abundance ratios smaller than solar neighborhood stars of the same metallicity ($[Fe/H]$ between -1.0 and -0.5, approximately), while others like O and Mg are only slightly deficient. If the LMC clusters follow the same abundance patterns as the field stars, then $[Ca/Fe] \sim -0.3$, which is different from both solar-scaled ($[Ca/Fe] = 0$) and empirical models at low Z ($[Ca/Fe] \sim +0.4$). For O and Mg, however, the empirical libraries should provide a good match.

In the spectral range that we are fitting, ages are mainly determined by the Balmer series and break, which are little affected by variations of $[\alpha/Fe]$, and thus the mismatch between the data and models does not affect significantly our age estimates. The metallicity, however, could be more affected. The most Z-dependent features in our spectra are the G band, CaII H+K, and Fe lines (e.g. Fe4383, Fe4045). Because the G band depends mainly on oxygen and iron abundances, and the LMC $[O/Fe]$ ratio follows the Galactic distribution, the band should be well fitted by the models. In contrast, given the difference between data and models in $[Ca/Fe]$, one would expect that models that fit well the CaII H+K lines may fail to fit the Fe lines, or vice-versa. We have inspected the fit residuals on the Ca and Fe lines, finding that for most SCs the best model fits well the two sets of lines. An exception is NGC 1651, which shows stronger Feλ4383 than any of the models that fit well the CaII H+K lines and G band.

Overall, we are unable to identify clear signatures of the effect of the mismatch in abundance pattern between models and our SC data. A broader spectral coverage (preferably extending to the CaII triplet, which is strongly affected by the $[Ca/Fe]$ ratio; Coelho et al. 2007), and a higher spectral resolution should reveal signs of this inconsistency. Models and methods which open Z into elemental abundances have appeared in the recent literature. For instance, Graves & Schiavon (2008) present a method to derive elemental abundances based on Lick indices, while methods to estimate $[\alpha/Fe]$ with full spectral fits have been presented by Prugniel et al. (2007) and Walcher et al. (2009), both based on the Coelho et al. (2007) models for α-enhanced SSPs. These more ambitious methodologies are still in their early days, and progress is expected in the coming years.

7.3 Age-metallicity relation for LMC clusters

In this section we discuss the capability of the models and the method to reproduce the age-metallicity relation for LMC clusters. Fig. 15a shows the age-metallicity relation using the data from the literature, as listed in columns 3 and 4 of Table 1. The plot also includes data for 15 intermediate-age SCs from Kerber et al. (2007), who determine the physical properties from modelling of HST CMDs. Some of their SCs are in common with this work. The literature data show

a gap in age and in metallicity on the LMC clusters, in the $3 \leqslant t \leqslant 10$ Gyr, and $-0.7 \leqslant \log Z/Z_\odot \leqslant -1.5$ intervals (Olszewski et al. 1991; Girardi et al 1995; MacKey & Gilmore 2003). So far, only the cluster ESO 121SC-03 was found in the t-Z gap (Geisler et al. 1997). This gap has been interpreted as a consequence of the history of SC formation in the LMC: two bursts with a significant enrichment in between the two episodes. This result is reflected in panel a of Fig. 15 except for five points corresponding to the young and intermediate age clusters NGC 1818, NGC 1866, NGC 2133, NGC 2134 and NGC 2214. The metallicities of these clusters are from Sangar & Pandei (1989) and Seggeswi & Ritcher (1989), and these are clearly underestimated.

Panels b to f of Fig. 15 show the t-Z relation obtained here for each set of models. STELIB-based models produce results that are very inconsistent with the t-Z relation. The metallicity is underestimated for most of the clusters, which, as a consequence of the t-Z degeneracy, move the intermediate-age SCs towards older ages, filling the age gap. The problem is even worse for young clusters, whose estimated metallicities come out severely underestimated. These conclusions are independent on the evolutionary tracks and the IMF, and are clearly a consequence of the lack of truly metal poor stars in the stellar library. However, as already pointed out (see Fig. 13), the ages are not so badly predicted.

Fits with the GRANADA models produce metallicities for young and intermediate-age clusters which are consistent with the average metallicity $\log Z/Z_\odot = -0.5$ obtained by Kerber et al. (2007). However, because of the lack of predictions for $\log Z/Z_\odot < -0.7$, these models not only fail to match the metallicity of the old metal poor SCs, but severely underestimate their ages.

The V00s models produce a very clean correlation between t and Z (with the already explained exception of NGC 1818, the outlier in Fig. 15e), but the relation indicates a continuous enrichment and no age gap. The reason is that the clusters NGC 1651, NGC 1795 and NGC 2121 are ~ 0.4 dex younger that the literature age. It has been argued that Padova 1994 isochrones are better than the Padova 2000 isochrones (used in the V00s models) because the latter provide older ages than expected for elliptical galaxies (BC03), which might explain why these clusters are 0.4–0.5 dex older with the V00s models than in the literature. The metallicities derived for these SCs are also incompatible with those in the literature: The fitted values are 0.7–1 dex smaller than in the literature. As usual, a positive difference in t implies a negative difference in Z.

CB94c provides results that are in very good agreement with the LMC t-Z relation. The gap in age and metallicity is reproduced, and intermediate age clusters have metallicity around $\log Z/Z_\odot = -0.5$. However, the younger SCs are very metal rich. The consistency of this result with data in the literature is difficult to evaluate considering the difficulty to derive metallicity in very young clusters.

7.4 Precision on age and metallicity

We now discuss the precision with which spectral fits using different models determine the physical properties of a stellar population. Formal (PDF-based) errors on the determinations of the age, and metallicity were listed in Tables 3–8.
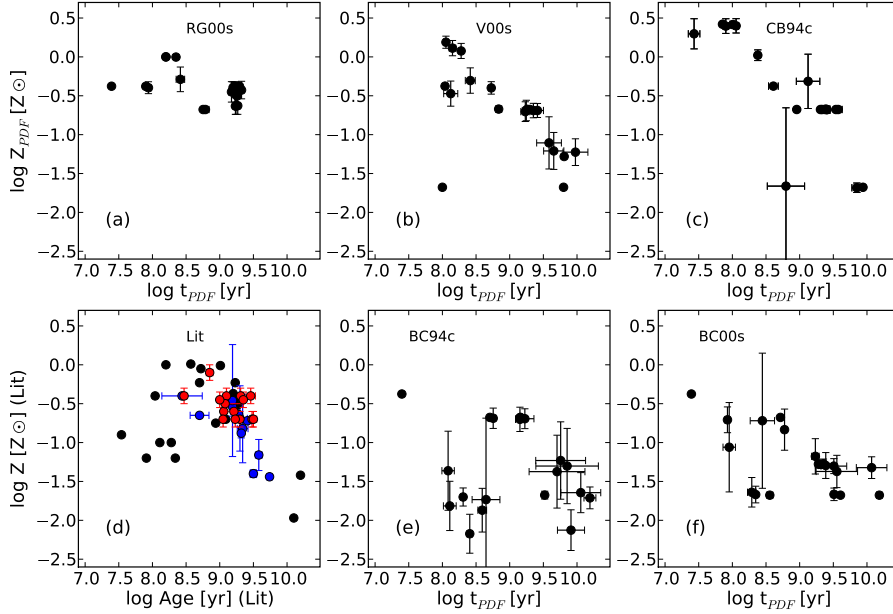
Figure 15. Age-metallicity relation for LMC clusters. Panels a to c (top, from left to right) and e and f (middle and right bottom), show results from STARLIGHT fits. Panel d (bottom left) shows the results from the literature: the Kerber et al. (2007) are plotted in red, LR03 are in blue, and the results listed in Table 1 from the S-CMD calibration and CaII lines are in black.

As we have discussed (Figs. 4 and 7) these errors are different for each set of models, but on average they are 0.07 and 0.13 dex for age and metallicity, respectively. However, we cannot consider these values as representative of the accuracy of t and Z estimates from spectral fits. In fact, because of the large number of degrees of freedom ($N_{dof} \sim 60$), in many cases the formal uncertainty is so unrealistically small that they are not even listed (the ± 0.00 entries in Tables 3–8).

A first estimate of the accuracy of the t and Z determinations through spectral fits can be done comparing the results obtained with different models. For this purpose we have computed the mean t and Z for each cluster and the dispersion of the different models results with respect to the global mean. For the whole sample, the average rms dispersion considering only one of the STELIB models (BC94c), plus the MILES (CB94c and V00s) and GRANADA (RG00s) models is 0.17 and 0.50 dex for t and Z, respectively. Because we have found that STELIB underestimates Z, we have recomputed these values excluding the STELIB results. In this case, the rms is 0.14 and 0.29 dex for t and Z, respectively. We have also tested how this precision depends on the age of the cluster. We find an rms of 0.08 dex in t for clusters younger than 1 Gyr, and 0.16 dex for older ones. The metallicity, however, has a similar precision for all ages. This is not unexpected, because for young clusters it is difficult to constrain Z, but the old clusters analyzed here are mainly metal poor, for which is also difficult to constraint Z.

We can also estimate the precisions in t and Z from the comparison between the values estimated with STARLIGHT
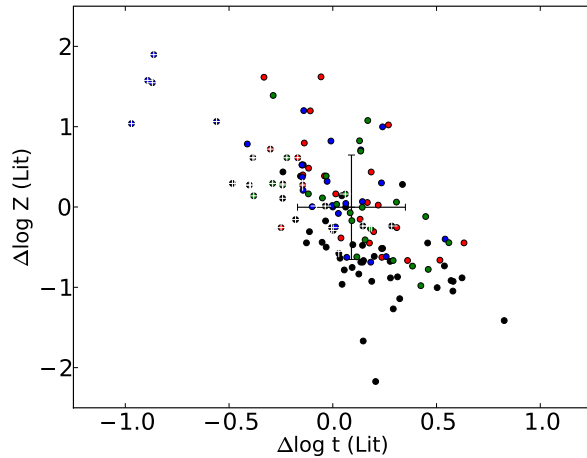
Figure 16. Relation between age and metallicity "errors", defined as the logarithmic differences between the spectral fitting and the literature values. The cross marks the position of the mean deviation, and the length of the cross is the rms of the distributions. STELIB models (only BC00s, and BC94c) results are plotted in black, CB94c models in red, RG00s models in blue, and V00s models in green circles. Low metallicity clusters are marked by a white cross on top the circle.

and those in the literature (Table 1). In principle, this provides a more absolute measure than the model-to-model internal variations used above. The deviations between our $\log t$ and $\log Z/Z_\odot$ estimates and the literature values are plotted against each-other in Fig. 16. The rms of these dis-

tributions are plotted with a cross 0.3 dex wide in $\log t$ and 0.7 dex wide in $\log Z/Z_\odot$. These cannot be considered the precision of the models because these quantities reflect too the error associated to the literature values, which can be very uncertain. For example, in Fig. 15a there are five young clusters that are completely off the age-metallicity relation of the LMC. Moreover, for many clusters, the ages have been estimated using the S-CMD calibration by Girardi et al. (1995), which by itself introduces 0.137 dex uncertainty in age. Recently, Pessev et al. (2008) have derived a new S-CMD calibration using the CMD results from Kerber et al. (2007). For the clusters that are in common, Kerber et al derive older ages than Girardi et al. So, the Pessev et al calibration is offset with respect to the Girardi et al by 0.235 dex. The STARLIGHT ages are also older than the literature values, most of which come from the Girardi et al calibration, but the detected offset towards older ages is only 0.09 dex on average, lower than the offset found by Pessev et al. Hence, the literature data do not seem as solid as desirable to be used as fiducial reference values.

Bearing in mind these caveats, we have computed the statistics of the difference between our t and Z values, averaged over the CB94c, RG00s and V00s models, with respect to the literature data. This results in an rms difference of 0.15 dex in age and 0.36 dex in metallicity.

In summary, the precision (or consistency between models and literature data) to constraint the age is ~ 0.1–0.2 dex in age and ~ 0.3–0.4 dex in metallicity.

8 SUMMARY AND CONCLUSIONS

This paper closes our empirical tests of modern spectral models for stellar populations. This study started in Paper I, where technical aspects of spectral fitting of SCs and the derivation of age, metallicity and extinction estimates were presented. In this paper we applied this methodology to spectra of 27 SCs from LR03 spanning a wide range of ages and metallicities. These data were fitted with seven versions of high resolution spectral models presently available: Galaxev with STELIB and MILES, SED@ with GRANADA, and Vazdekis with MILES stellar libraries. Extensive comparisons of the quality of the spectral fits and the inferred physical properties were presented, in an effort to map the pros and cons of each set of evolutionary synthesis models and thus provide useful feedback for model makers, as well as guidance to the ever growing community of users of such models.

Our main conclusions may be summarized as follows:

(i) Models based on the MILES and GRANADA libraries yield slightly better spectral fits, as long as their age and metallicity limitations are observed. Overall, however, all the models are able to produce very good quality fits.

(ii) The formal uncertainties in age are on average less than 0.1 dex. The metallicity and extinction PDFs are broader than that of the age, indicating that t is better constrained than Z and A_V. This is at least in part a consequence of small spectral range used here to perform the fits. Uncertainties are on average smaller for MILES and GRANADA models than for STELIB ones. With the former two models we obtain $\sigma(\log t) = 0.05$ dex, $\sigma(\log Z/Z_\odot) = 0.1$ dex, and $\sigma(A_V) = 0.06$ mag, while with the latter these average values increase to 0.1 dex, 0.2 dex and 0.09 mag, respectively.

(iii) Ages correlate very well with the data in the literature. Ages derived from our spectral fits are 0.09 dex larger than the S-CMD ages.

(iv) Metallicities derived from spectral fits correlate poorly with the literature data. This happens due to a combination of the intrinsic difficulty in deriving Z (specially over the limited spectral range studied here), the coarseness of the grids in Z, plus the inhomogeneity and uncertainties in the literature values.

(v) Fits with STELIB-based models produce metallicities systematically smaller by about 0.6 dex with respect to what is found with other models. Thus, STELIB/BC03 based results will need revision. In particular, stellar metallicities estimated with BC03 models will probably be revised upwards. However, ages are probably right.

(vi) Extinctions derived are small, as expected for the clusters in our sample.

(vii) Metal poor clusters are poorly fitted by the GRANADA models as a consequence of lack of predictions for Z below 0.2 solar. The error on the age estimated by the other models is also higher than the average precision reflecting too the difficulty of derived ages for metal poor clusters if the Balmer lines are contaminated by the contribution of blue stars in the horizontal branch.

(viii) The precision (or consistency) of the models to determine the age and metallicity is 0.17 and 0.5 dex (rms of the models with respect to the mean). If STELIB are excluded, the consistency of the models is better, with an rms of 0.1 and 0.3 dex for age and metallicity, respectively.

(ix) Model-to-model dispersions in derived t and Z values are about 0.2 and 0.5 dex, respectively. Removing models based on STELIB these values reduce to 0.1 dex in age and 0.3 dex in metallicity. Similar differences are found when comparing the spectral fit results to the literature values for t and Z.

These conclusions indicate the relevance to have models with isochrones covering a big range in metallicity and stellar libraries covering a big range in the stellar parameters (T_{eff}, gravity, and metallicity).

REFERENCES

Beasley M. A., Hoyle F., Sharples R. M., 2002, MNRAS, 336, 168

Bertelli G., Bressan A., Chiosi C., Fagotto F., Nasi E., 1994, A&AS, 106, 275

Bertone, E., Buzzoni, A., Chávez, M., & Rodríguez-Merino, L. H. 2008, A&A, 485, 823

Bica E., Alloin D., 1986, A&A, 162, 21

Bica E., Clariá, J. J., Dottori H., 1992, AJ, 103, 1859

Bica E., Clariá J. J., Dottori H., Santos J .F. C. Jr., Piatti A. E., 1996, ApJS, 102, 57

Bruzual G., Charlot S., 2003, MNRAS, 344, 1000

Cerviño M., Luridiana V., 2006, A&A, 413, 145

Cerviño M., Luridiana V., 2004, A&A, 451, 475

Cerviño M., Luridiana V., Castander F. J., 2000, A&A, 360, 5

Chabrier G., 2003, PASP, 115, 763

Coelho, P., Bruzual, G., Charlot, S., Weiss, A., Barbuy, B., Ferguson, J. W., 2007, MNRAS, 382, 498

Cid Fernandes R., Mateus A., Sodré L., Stasińska G., Gomes J. M., 2005, MNRAS, 358, 363

Cid Fernandes R., 2007, on Stellar Populations as Building Blocks of Galaxies, Proceedings of IAU Symposium 241. Edited by A. Vazdekis and R. F. Peletier. Cambridge: Cambridge University Press, p. 461-469

Cid Fernandes R., González Delgado R. M., 2009, this volumen

Charlot S., Bruzua, G., 2009, in prep.

Dirsch B., Richtler T., Gieren W. P., Hilker M., 2000, A&A, 360, 133

Elson R. A. W., Fall S. M., 1988, AJ, 96, 1383

de Grijs R., Anders P., 2006, MNRAS, 366, 295

Geisler D., Bica E., Dottori H., Claria J. J., Piatti A. E., Santos J. F. C. Jr., 1997, AJ, 114, 1920

Girardi, L., Chiosi, C., Bertelli, G., & Bressan, A. 1995, A&A, 298, 87

Girardi L., Bressan A., Bertelli G., Chiosi C., 2000, A&A, 141, 371

Girardi L., Bertelli G., Bressan A., Chiosi C., Groenewegen M. A. T., Marigo P., Salasnich B., Weiss A., 2002, A&A, 391, 195

Geisler D., Bica E., Dottori H., Clariá J. J., Piatti A. E., Santos J. F. C. Jr., 1997, AJ, 114, 1920

Graves, G. J., & Schiavon, R. P. 2008, ApJS, 177, 446

González Delgado R. M., Leitherer C., Heckman T., Cerviño M., 1997, ApJ, 483, 705

González Delgado R.M., Leitherer C., Heckman T., 1999, ApJS, 125, 489

González Delgado R. M., Cerviño M., Martins L. P., Leitherer C., Hauschildt P. H., 2005, MNRAS, 357, 945

González Delgado R. M., 2009, ApSS, in press

Hauschildt P. H., Baron, E., 1999, J. Comp. Appl. Math., 102, 41

Hubeny I., Lanz T., Jeffery C. S., 1995, SYNSPEC- A Users Guide

Lancon, A., Mouhcine, M., 2000, in "Massive Stellar Clusters", Proceedings of the international workshop held in Strasbourg, France, November 8-11, 1999. Eds.: A. Lancon, and C. Boily, Astronomical Society of the Pacific Conference Series., p.34

Lanz T., Hubeny I., 2003, ApJS, 146, 417

Le Borgne J. -F., et al., 2003, A&A, 402, 433

Le Borgne D., Rocca-Volmerange B., Prugniel P., Lançon A., Fioc M., Soubiran C., 2004, A&A, 425, 881

Leonardi A. J., Rose J. A., 2003, ApJ, 126, 1811

Kerber L. O., Santiago B. X., Brocato, E., 2007, A&A, 462, 139

Koleva M., Prugniel Ph., Ocvirk P., Le Borgne D., Soubiran C., 2008, MNRAS, 385, 1998

Kurucz R. L., 1993, Kurucz CD-ROM 13, ATLAS9 Stellar Atmosphere Programs and 2 km/s Grid (Cambridge:SAO)

Maíz-Apellániz J., 2009, ApJ, in press

Martins L. P., González Delgado R. M., Leitherer C., Cerviño M., Hauschildt P. H., 2005, MNRAS, 358, 49

Martins L. P., Coelho, P., 2007, MNRAS, 381, 1329

Meylan G., 2003, in "New Horizons in Globular Cluster Astronomy", ASP Conference Proceedings, eds. G. Piotto, G. Meylan, S.G. Djorgovski and M. Riello, Vol. 296, p.17

McLaughlin D. E., van der Marel R. P., 2005, ApJS, 161, 304

McWilliam, A., Rich, R. M., 1994, ApJS, 91, 749

Olsen K. A. G., Hodge P. W., Mateo M., Olszewski E. W., Schommer R. A., Suntzeff N. B., Walker A. R., 1998, MNRAS, 300, 665

Olszewski E. W., Schommer R. A., Suntzeff N. B., Harris H. C., 1991, AJ, 101, 515

Panter, B., Jimenez, R., Heavens, A. F., & Charlot, S. 2007, MNRAS, 378, 1550

Pompéia, L., Hill, V., Spite, M., Cole, A., Primas, F., Romaniello, M., Pasquini, L., Cioni, M.-R., Smecker Hane, T., 2008, A&A, 480, 379

Prugniel, P., Koleva, M., Ocvirk, P., Le Borgne, D., Soubiran, C., 2007, in "Stellar Populations as Building Blocks of Galaxies", Proceedings of IAU Symposium 241. Edited by A. Vazdekis and R. F. Peletier. Cambridge: Cambridge University Press, p.68

Prugniel P., Soubiran C., 2004, astro-ph/0409214

Rodríguez-Merino L. H., Chavez M., Bertone E., Buzzoni A., 2005, ApJ, 626, 411

Sagar R., Pandey A. K., 1989, A&AS, 79, 407

Salpeter E. E., 1955, ApJ, 121, 161

Sánchez-Blázquez P., et al., 2006, MNRAS, 371, 703

Santos J. F. C., Jr., Clariá J. J., Ahumada A. V., Bica E., Piatti A. E., Parisi M. C., 2006, A&A, 448, 1023

Schiavon, R. P., Rose, J. A., Courteau, S., MacArthur, L. A., 2005, ApJS, 160, 163

Seggewise W., Richtler T., 1989, in Recent Developments of Magellanic Cloud Research, ed. K. S. de Boer, F. Spite, and Stasinska (Meudon: Obs. Paris), 45

Tantalo, R., Chiosi, C., 2004, MNRAS, 353, 917

Tinsley B. M., 1968, ApJ, 151, 547

Thomas, D., Maraston, C., 2003, A&A, 401, 429

Thomas, D., Maraston, C., Korn, A., 2004, MNRAS, 351, L19

Valdes F., Gupta R., Rose J. A., Singh H. P., Bell D. J., ApJS, 152, 251

Vazdekis A., 1999, ApJ, 513, 224

Vazdekis A., et al., 2009, MNRAS, submitted

Walcher, C. J., Coelho, P., Gallazzi, A., Charlot, S., 2009, MNRAS, 398, L44

Wolf M. J., Drory N., Gebhardt K., Hill G. J., 2007, ApJ,

  655, 179
Worthey, G., Faber, S. M., & Gonzalez, J. J. 1992, ApJ,
 398, 69
Zaritsky D., Harris J., Thompson L., 1997, AJ, 114, 1002
Zaritsky D., Harrison J., 2004, ApJ, 604, 167

Table 3. Results for CB94c models

	Single population fits					Multi population fits				Bayesian estimates		
Cluster (1)	$\log t$ (2)	$\log Z/Z_\odot$ (3)	A_V (4)	$\overline{\Delta}$ (5)	δ_m (6)	$\overline{\log t_m}$ (7)	σ_m (8)	$\overline{\Delta}_m$ (9)	$\log T_m$ (%) (10)	$\log t$ (11)	$\log Z/Z_\odot$ (12)	A_V (13)
NGC 411	9.26	-0.68	0.17	2.4	0.09	9.26	0.26	2.3	9.26 (34)	9.26 ± 0.00	-0.68 ± 0.02	0.17 ± 0.04
NGC 416	9.51	-0.68	0.00	2.4	1.64	9.13	1.23	1.4	9.76 (25)	9.53 ± 0.07	-0.71 ± 0.17	0.02 ± 0.08
NGC 419	9.26	-0.68	0.15	2.0	0.49	9.19	0.53	1.6	8.96 (60)	9.24 ± 0.08	-0.64 ± 0.17	0.15 ± 0.04
NGC 1651	9.40	-0.68	0.14	4.1	0.07	9.42	0.42	4.0	9.57 (46)	9.40 ± 0.02	-0.68 ± 0.03	0.14 ± 0.09
NGC 1754	9.94	-1.68	0.29	2.5	0.11	9.75	0.96	2.3	9.95 (50)	9.94 ± 0.00	-1.68 ± 0.00	0.29 ± 0.05
NGC 1783	8.96	0.02	0.00	2.1	1.32	8.80	0.69	1.3	8.96 (28)	9.11 ± 0.17	-0.29 ± 0.35	0.14 ± 0.13
NGC 1795	9.41	-0.68	0.01	5.1	0.01	9.28	0.67	5.1	9.44 (43)	9.41 ± 0.04	-0.68 ± 0.05	0.11 ± 0.09
NGC 1806	9.32	-0.68	0.42	1.9	0.24	9.31	0.47	1.8	9.54 (34)	9.33 ± 0.01	-0.68 ± 0.00	0.42 ± 0.04
NGC 1818	7.38	0.42	0.57	1.6	0.44	7.35	0.73	1.3	6.52 (30)	7.41 ± 0.07	0.35 ± 0.16	0.48 ± 0.19
NGC 1831	8.66	-0.38	0.06	2.1	0.17	8.63	0.15	2.0	8.51 (57)	8.61 ± 0.07	-0.38 ± 0.01	0.15 ± 0.14
NGC 1846	9.30	-0.68	0.24	3.0	0.11	9.27	0.49	2.8	9.01 (42)	9.31 ± 0.00	-0.68 ± 0.01	0.25 ± 0.07
NGC 1866	8.01	0.42	0.56	1.4	0.04	8.06	0.26	1.4	8.06 (49)	8.01 ± 0.00	0.42 ± 0.03	0.56 ± 0.04
NGC 1978	9.54	-0.68	0.16	1.7	0.11	9.46	0.58	1.6	9.63 (44)	9.54 ± 0.02	-0.68 ± 0.00	0.15 ± 0.04
NGC 2010	8.06	0.42	0.10	1.8	0.04	8.09	0.17	1.7	8.06 (61)	8.05 ± 0.03	0.41 ± 0.07	0.13 ± 0.08
NGC 2121	9.60	-0.68	0.13	4.6	0.16	9.66	1.09	4.3	10.30 (25)	9.57 ± 0.06	-0.68 ± 0.01	0.17 ± 0.10
NGC 2133	8.36	0.02	0.28	1.8	0.02	8.38	0.05	1.7	8.36 (44)	8.38 ± 0.03	0.02 ± 0.10	0.19 ± 0.11
NGC 2134	9.01	-2.28	0.00	1.5	0.08	8.96	0.18	1.4	8.96 (46)	8.87 ± 0.22	-1.94 ± 0.81	0.06 ± 0.07
NGC 2136	7.91	0.42	0.57	1.6	0.12	7.98	0.37	1.5	7.96 (42)	7.90 ± 0.03	0.41 ± 0.07	0.60 ± 0.08
NGC 2203	9.40	-0.68	0.43	2.8	0.16	9.44	0.96	2.6	8.96 (39)	9.39 ± 0.02	-0.67 ± 0.04	0.42 ± 0.09
NGC 2210	9.83	-1.68	0.21	1.5	0.45	9.90	1.14	1.2	10.28 (21)	9.86 ± 0.09	-1.69 ± 0.09	0.20 ± 0.05
NGC 2213	9.38	-0.68	0.32	2.6	0.36	9.45	0.43	2.3	8.96 (36)	9.37 ± 0.02	-0.68 ± 0.02	0.32 ± 0.06
NGC 2214	7.86	0.42	0.14	1.1	0.04	7.84	0.04	1.1	7.86 (46)	7.85 ± 0.01	0.42 ± 0.00	0.15 ± 0.04
NGC 2249	8.96	-0.68	0.00	2.1	0.18	8.81	0.46	1.9	8.96 (80)	8.96 ± 0.00	-0.68 ± 0.01	0.01 ± 0.02
47Tuc	9.99	-0.38	0.00	2.9	0.43	9.87	0.88	2.5	10.01 (24)	9.98 ± 0.03	-0.37 ± 0.03	0.02 ± 0.02
M 15	9.86	-1.68	0.04	1.6	1.41	9.31	1.48	1.0	9.65 (19)	9.85 ± 0.00	-1.68 ± 0.01	0.05 ± 0.03
M 79	9.93	-1.68	0.00	1.4	0.16	9.89	0.74	1.2	9.95 (77)	9.93 ± 0.02	-1.68 ± 0.00	0.01 ± 0.01
NGC 1851	9.63	-0.68	0.00	2.6	2.42	9.47	1.04	1.5	9.76 (69)	9.61 ± 0.05	-0.68 ± 0.00	0.01 ± 0.01

Table 4. Results for RG00s models

	Single population fits					Multi population fits					Bayesian estimates		
Cluster (1)	$\log t$ (2)	$\log Z/Z_\odot$ (3)	A_V (4)	$\overline{\Delta}$ (5)	δ_m (6)	$\overline{\log t_m}$ (7)	σ_m (8)	$\overline{\Delta}_m$ (9)	$\log T_m$ (%) (10)		$\log t$ (11)	$\log Z/Z_\odot$ (12)	A_V (13)
NGC 411	9.20	-0.68	0.00	2.8	0.38	8.88	0.73	2.4	9.15 (50)		9.13 ± 0.07	-0.52 ± 0.17	0.06 ± 0.06
NGC 416	9.30	-0.38	0.00	4.1	3.74	8.55	1.25	1.9	6.80 (34)		9.28 ± 0.02	-0.38 ± 0.00	0.01 ± 0.01
NGC 419	9.05	-0.38	0.10	2.5	0.90	8.74	0.81	1.9	8.90 (34)		9.06 ± 0.03	-0.39 ± 0.07	0.09 ± 0.04
NGC 1651	9.20	-0.38	0.00	4.6	0.15	8.89	0.86	4.3	9.35 (60)		9.24 ± 0.04	-0.50 ± 0.15	0.04 ± 0.04
NGC 1754	9.20	-0.38	0.00	5.2	5.73	8.41	1.25	2.1	6.80 (38)		9.22 ± 0.03	-0.39 ± 0.06	0.02 ± 0.02
NGC 1783	9.15	-0.38	0.00	2.4	0.43	8.86	0.79	2.0	9.30 (30)		9.19 ± 0.05	-0.49 ± 0.15	0.03 ± 0.03
NGC 1795	9.30	-0.68	0.00	5.6	0.21	8.90	0.98	5.4	9.15 (62)		9.25 ± 0.04	-0.53 ± 0.15	0.05 ± 0.05
NGC 1806	9.25	-0.68	0.09	2.5	0.35	8.94	0.79	2.3	9.15 (49)		9.25 ± 0.02	-0.65 ± 0.08	0.10 ± 0.05
NGC 1818	7.40	-0.38	0.44	1.2	0.07	7.45	0.35	1.2	7.35 (55)		7.39 ± 0.02	-0.38 ± 0.03	0.45 ± 0.05
NGC 1831	8.75	-0.68	0.01	1.5	0.13	8.76	0.14	1.4	8.80 (73)		8.75 ± 0.01	-0.68 ± 0.00	0.03 ± 0.03
NGC 1846	9.25	-0.68	0.00	3.2	0.28	8.86	0.84	3.1	9.15 (74)		9.24 ± 0.03	-0.65 ± 0.08	0.04 ± 0.04
NGC 1866	8.20	0.00	0.29	1.4	0.46	8.09	0.52	1.2	8.30 (85)		8.20 ± 0.00	0.00 ± 0.00	0.29 ± 0.03
NGC 1978	9.30	-0.38	0.00	2.6	0.47	8.94	0.91	2.3	9.35 (76)		9.29 ± 0.02	-0.38 ± 0.02	0.03 ± 0.03
NGC 2010	8.20	0.00	0.01	1.8	0.06	8.15	0.44	1.7	8.30 (86)		8.20 ± 0.01	0.00 ± 0.00	0.03 ± 0.03
NGC 2121	9.40	-0.68	0.00	5.3	0.21	9.11	1.05	4.8	9.75 (23)		9.33 ± 0.05	-0.46 ± 0.14	0.11 ± 0.09
NGC 2133	8.35	0.00	0.26	1.7	0.11	8.40	0.15	1.6	8.35 (46)		8.35 ± 0.01	0.00 ± 0.02	0.26 ± 0.05
NGC 2134	8.45	-0.38	0.05	1.3	0.08	8.46	0.16	1.2	8.50 (93)		8.39 ± 0.07	-0.24 ± 0.18	0.14 ± 0.11
NGC 2136	7.95	-0.38	0.60	1.6	0.04	7.94	0.06	1.5	7.90 (61)		7.95 ± 0.05	-0.41 ± 0.10	0.62 ± 0.10
NGC 2203	9.30	-0.68	0.11	3.0	0.27	9.03	0.81	2.7	9.15 (42)		9.27 ± 0.04	-0.55 ± 0.15	0.12 ± 0.07
NGC 2210	9.20	-0.38	0.00	6.0	11.20	8.19	1.20	1.7	6.80 (43)		9.20 ± 0.02	-0.41 ± 0.10	0.02 ± 0.02
NGC 2213	9.30	-0.68	0.00	2.7	0.22	9.04	0.73	2.5	9.15 (66)		9.27 ± 0.03	-0.65 ± 0.08	0.04 ± 0.03
NGC 2214	7.90	-0.38	0.15	1.2	0.00	7.90	0.00	1.2	7.90 (100)		7.90 ± 0.01	-0.38 ± 0.04	0.14 ± 0.03
NGC 2249	8.80	-0.68	0.00	2.1	0.59	8.71	0.38	1.7	8.95 (57)		8.79 ± 0.05	-0.68 ± 0.00	0.06 ± 0.14
47Tuc	9.95	-0.68	0.00	4.3	0.14	9.85	0.90	4.2	10.10 (91)		9.90 ± 0.08	-0.60 ± 0.13	0.06 ± 0.06
M 15	9.20	-0.38	0.00	7.0	12.45	7.96	1.20	1.8	6.80 (52)		9.14 ± 0.27	-0.41 ± 0.14	0.06 ± 0.20
M 79	9.20	-0.38	0.00	6.9	12.62	8.40	1.21	1.9	6.80 (36)		9.21 ± 0.03	-0.43 ± 0.11	0.02 ± 0.02
NGC 1851	9.30	-0.38	0.00	4.2	2.38	8.82	1.18	2.4	9.50 (50)		9.31 ± 0.02	-0.38 ± 0.01	0.02 ± 0.02

Table 5. Results for BC94c models

	Single population fits					Multi population fits				Bayesian estimates		
Cluster (1)	$\log t$ (2)	$\log Z/Z_\odot$ (3)	A_V (4)	$\overline{\Delta}$ (5)	δ_m (6)	$\overline{\log t_m}$ (7)	σ_m (8)	$\overline{\Delta}_m$ (9)	$\log T_m$ (%) (10)	$\log t$ (11)	$\log Z/Z_\odot$ (12)	A_V (13)
NGC 411	9.38	-1.68	0.58	2.8	0.00	9.41	0.18	2.8	9.36 (62)	9.38 ± 0.04	-1.67 ± 0.05	0.58 ± 0.05
NGC 416	10.09	-1.68	0.37	2.2	0.03	10.02	0.39	2.1	10.30 (35)	9.98 ± 0.13	-1.68 ± 0.00	0.44 ± 0.10
NGC 419	9.01	-0.68	0.55	2.0	0.66	8.83	0.66	1.5	8.91 (49)	9.18 ± 0.17	-1.17 ± 0.50	0.57 ± 0.04
NGC 1651	9.21	-0.68	0.08	4.2	0.15	8.89	0.84	3.9	9.30 (39)	9.71 ± 0.42	-1.38 ± 0.47	0.47 ± 0.28
NGC 1754	10.29	-1.68	0.00	2.6	0.17	9.80	1.16	2.4	10.30 (66)	10.20 ± 0.09	-1.75 ± 0.19	0.10 ± 0.10
NGC 1783	9.51	-1.68	0.73	2.2	0.04	9.72	0.40	2.2	9.44 (64)	9.52 ± 0.00	-1.68 ± 0.06	0.73 ± 0.06
NGC 1795	10.30	-1.68	0.38	5.1	0.00	10.28	0.14	5.1	10.30 (98)	10.06 ± 0.29	-1.67 ± 0.28	0.51 ± 0.21
NGC 1806	9.16	-0.68	0.31	2.1	0.59	8.89	0.67	1.7	9.28 (38)	9.16 ± 0.01	-0.68 ± 0.04	0.31 ± 0.05
NGC 1818	7.40	-0.38	0.34	1.9	0.00	7.40	0.01	1.9	7.40 (86)	7.40 ± 0.03	-0.38 ± 0.00	0.35 ± 0.09
NGC 1831	8.71	-0.68	0.26	2.0	0.00	8.71	0.00	2.0	8.71 (100)	8.71 ± 0.02	-0.68 ± 0.01	0.26 ± 0.05
NGC 1846	9.16	-0.68	0.13	3.1	0.26	8.84	0.76	2.9	8.86 (37)	9.15 ± 0.07	-0.70 ± 0.16	0.18 ± 0.14
NGC 1866	8.31	-1.68	0.36	2.2	0.00	8.31	0.00	2.2	8.31 (100)	8.31 ± 0.04	-1.72 ± 0.16	0.38 ± 0.10
NGC 1978	9.26	-0.68	0.16	2.4	0.52	8.93	0.92	1.8	9.28 (49)	9.86 ± 0.46	-1.31 ± 0.48	0.51 ± 0.27
NGC 2010	8.41	-2.28	0.19	2.4	0.01	8.46	0.07	2.4	8.51 (64)	8.41 ± 0.04	-2.22 ± 0.21	0.13 ± 0.09
NGC 2121	9.34	-0.68	0.16	5.2	0.26	9.08	1.26	4.5	9.30 (29)	9.76 ± 0.37	-1.24 ± 0.50	0.55 ± 0.35
NGC 2133	8.76	-2.28	0.17	2.5	0.01	8.76	0.13	2.5	8.86 (58)	8.66 ± 0.20	-1.77 ± 1.03	0.20 ± 0.12
NGC 2134	8.61	-1.68	0.00	1.9	0.02	8.63	0.09	1.9	8.66 (91)	8.61 ± 0.07	-1.96 ± 0.30	0.10 ± 0.09
NGC 2136	8.11	-1.68	0.51	2.3	0.02	8.22	0.34	2.3	8.21 (61)	8.09 ± 0.10	-1.40 ± 0.53	0.39 ± 0.13
NGC 2203	9.21	-0.68	0.37	3.0	0.23	9.04	0.88	2.6	9.28 (53)	9.23 ± 0.14	-0.69 ± 0.13	0.37 ± 0.09
NGC 2210	10.13	-2.28	0.31	2.5	0.59	8.95	1.66	2.1	6.52 (27)	9.96 ± 0.17	-2.19 ± 0.21	0.33 ± 0.11
NGC 2213	9.16	-0.68	0.22	2.3	0.19	8.98	0.70	2.1	9.28 (57)	9.16 ± 0.00	-0.68 ± 0.00	0.22 ± 0.05
NGC 2214	8.26	-2.28	0.00	2.3	0.19	8.21	0.56	2.2	8.36 (78)	8.15 ± 0.11	-1.93 ± 0.34	0.05 ± 0.05
NGC 2249	8.76	-0.68	0.30	2.2	0.08	8.67	0.41	2.1	8.76 (55)	8.76 ± 0.05	-0.70 ± 0.18	0.30 ± 0.06
47Tuc	9.90	-0.38	0.00	2.9	0.02	9.85	0.52	2.9	9.95 (42)	9.86 ± 0.04	-0.38 ± 0.00	0.08 ± 0.06
M 15	10.00	-2.28	0.22	2.5	1.65	8.56	1.66	1.6	8.01 (22)	9.98 ± 0.08	-2.28 ± 0.01	0.22 ± 0.07
M 79	9.68	-1.68	0.00	1.9	0.17	9.73	0.64	1.7	10.30 (16)	9.93 ± 0.28	-1.94 ± 0.30	0.02 ± 0.02
NGC 1851	9.93	-1.68	0.60	2.7	0.00	9.98	0.09	2.7	9.95 (77)	9.96 ± 0.04	-1.68 ± 0.00	0.58 ± 0.07

Table 6. Results for BBC00c models

	Single population fits					Multi population fits				Bayesian estimates		
Cluster (1)	$\log t$ (2)	$\log Z/Z_\odot$ (3)	A_V (4)	$\overline{\Delta}$ (5)	δ_m (6)	$\overline{\log t_m}$ (7)	σ_m (8)	$\overline{\Delta}_m$ (9)	$\log T_m$ (%) (10)	$\log t$ (11)	$\log Z/Z_\odot$ (12)	A_V (13)
NGC 411	9.11	-1.28	0.60	2.6	0.12	9.03	0.48	2.5	8.66 (30)	9.13 ± 0.06	-1.30 ± 0.09	0.59 ± 0.06
NGC 416	10.04	-1.68	0.42	2.2	0.09	10.09	0.43	2.1	10.29 (54)	10.03 ± 0.07	-1.68 ± 0.00	0.44 ± 0.08
NGC 419	9.11	-1.28	0.59	1.6	0.17	9.09	0.41	1.5	9.01 (31)	9.11 ± 0.01	-1.28 ± 0.01	0.58 ± 0.03
NGC 1651	9.36	-1.28	0.36	4.0	0.13	9.18	0.74	3.9	9.57 (43)	9.42 ± 0.17	-1.31 ± 0.18	0.40 ± 0.16
NGC 1754	10.28	-1.68	0.02	2.3	0.13	10.05	0.78	2.2	10.30 (91)	10.24 ± 0.04	-1.68 ± 0.00	0.06 ± 0.05
NGC 1783	9.51	-1.68	0.78	2.0	0.00	9.52	0.13	2.1	9.54 (97)	9.52 ± 0.03	-1.67 ± 0.07	0.78 ± 0.06
NGC 1795	9.36	-1.28	0.31	5.0	0.07	9.01	0.98	4.9	9.54 (33)	9.70 ± 0.37	-1.45 ± 0.23	0.42 ± 0.20
NGC 1806	9.28	-1.28	0.64	2.1	0.40	9.12	0.62	1.8	9.57 (38)	9.28 ± 0.01	-1.28 ± 0.03	0.64 ± 0.05
NGC 1818	7.40	-0.38	0.34	1.9	0.00	7.40	0.01	1.9	7.40 (75)	7.39 ± 0.03	-0.38 ± 0.00	0.35 ± 0.09
NGC 1831	8.71	-0.68	0.32	2.0	0.00	8.72	0.02	1.9	8.71 (79)	8.72 ± 0.03	-0.68 ± 0.00	0.30 ± 0.06
NGC 1846	9.26	-1.28	0.49	3.0	0.11	9.26	0.72	2.9	9.51 (19)	9.24 ± 0.06	-1.18 ± 0.23	0.49 ± 0.07
NGC 1866	8.31	-1.68	0.43	2.1	0.00	8.31	0.01	2.1	8.31 (99)	8.30 ± 0.05	-1.66 ± 0.12	0.43 ± 0.09
NGC 1978	9.48	-1.28	0.49	2.2	0.31	9.21	0.85	1.8	9.57 (37)	9.51 ± 0.18	-1.30 ± 0.09	0.50 ± 0.07
NGC 2010	8.36	-1.68	0.02	2.4	0.02	8.36	0.11	2.4	8.31 (61)	8.35 ± 0.01	-1.67 ± 0.09	0.06 ± 0.06
NGC 2121	10.17	-1.28	0.19	4.9	0.11	9.62	1.27	4.5	10.30 (28)	10.12 ± 0.17	-1.29 ± 0.07	0.24 ± 0.16
NGC 2133	8.31	0.00	0.27	2.4	0.00	8.30	0.06	2.4	8.31 (75)	8.53 ± 0.18	-1.11 ± 0.82	0.19 ± 0.11
NGC 2134	8.61	-1.68	0.00	1.8	0.02	8.64	0.14	1.8	8.76 (55)	8.56 ± 0.05	-1.68 ± 0.00	0.07 ± 0.06
NGC 2136	7.91	-0.68	0.37	2.3	0.01	7.92	0.02	2.3	7.91 (74)	7.93 ± 0.04	-0.72 ± 0.20	0.35 ± 0.08
NGC 2203	9.36	-1.28	0.65	2.8	0.12	9.51	0.78	2.6	9.54 (20)	9.36 ± 0.02	-1.27 ± 0.06	0.65 ± 0.07
NGC 2210	9.63	-1.68	0.23	2.7	0.63	9.37	1.34	2.0	10.30 (38)	9.62 ± 0.02	-1.68 ± 0.00	0.21 ± 0.07
NGC 2213	9.30	-1.28	0.54	2.3	0.08	9.30	0.52	2.2	9.54 (32)	9.31 ± 0.00	-1.28 ± 0.01	0.54 ± 0.05
NGC 2214	7.86	-0.68	0.00	2.1	0.04	7.83	0.38	2.1	7.91 (88)	7.97 ± 0.09	-1.20 ± 0.56	0.08 ± 0.07
NGC 2249	8.81	-0.68	0.29	2.3	0.14	8.65	0.49	2.1	8.66 (37)	8.78 ± 0.04	-0.94 ± 0.30	0.43 ± 0.14
47Tuc	9.48	0.00	0.00	3.1	0.09	9.43	0.61	3.0	9.60 (33)	9.76 ± 0.15	-0.30 ± 0.15	0.10 ± 0.07
M 15	9.65	-1.68	0.12	2.7	1.53	8.73	1.42	1.6	6.56 (25)	9.64 ± 0.02	-1.68 ± 0.00	0.10 ± 0.06
M 79	9.68	-1.68	0.07	1.9	0.30	9.71	1.14	1.6	10.30 (59)	9.68 ± 0.01	-1.68 ± 0.00	0.07 ± 0.04
NGC 1851	9.95	-1.68	0.63	2.7	0.02	10.02	0.14	2.7	9.95 (80)	9.95 ± 0.01	-1.67 ± 0.05	0.62 ± 0.10

Table 7. Results for BBC94s models

Cluster (1)	Single population fits					Multi population fits				Bayesian estimates		
	$\log t$ (2)	$\log Z/Z_\odot$ (3)	A_V (4)	$\overline{\Delta}$ (5)	δ_m (6)	$\overline{\log t_m}$ (7)	σ_m (8)	$\overline{\Delta}_m$ (9)	$\log T_m$ (%) (10)	$\log t$ (11)	$\log Z/Z_\odot$ (12)	A_V (13)
NGC 411	9.38	-1.68	0.57	2.8	0.00	9.39	0.14	2.8	9.36 (75)	9.37 ± 0.04	-1.67 ± 0.07	0.58 ± 0.05
NGC 416	10.11	-1.68	0.30	2.1	0.05	9.99	0.67	2.0	10.30 (42)	10.02 ± 0.13	-1.68 ± 0.00	0.37 ± 0.10
NGC 419	9.01	-0.68	0.55	2.0	0.57	8.89	0.45	1.5	8.91 (36)	9.16 ± 0.17	-1.14 ± 0.50	0.56 ± 0.04
NGC 1651	9.21	-0.68	0.07	4.1	0.14	8.92	0.80	3.9	9.30 (53)	9.54 ± 0.34	-1.29 ± 0.52	0.43 ± 0.31
NGC 1754	10.30	-2.28	0.18	2.4	0.08	9.67	1.41	2.4	10.30 (71)	10.24 ± 0.07	-2.07 ± 0.29	0.15 ± 0.10
NGC 1783	9.51	-1.68	0.71	2.2	0.03	9.67	0.38	2.2	9.44 (48)	9.51 ± 0.00	-1.68 ± 0.06	0.71 ± 0.05
NGC 1795	10.30	-1.68	0.29	5.1	0.01	10.22	0.30	5.1	10.30 (93)	10.05 ± 0.29	-1.71 ± 0.29	0.48 ± 0.22
NGC 1806	9.16	-0.68	0.30	2.1	0.65	8.80	0.87	1.7	9.28 (60)	9.16 ± 0.01	-0.68 ± 0.04	0.30 ± 0.05
NGC 1818	7.40	-0.38	0.34	2.0	0.00	7.40	0.00	2.0	7.40 (95)	7.39 ± 0.03	-0.38 ± 0.00	0.36 ± 0.09
NGC 1831	8.71	-0.68	0.26	2.0	0.00	8.71	0.00	2.0	8.71 (100)	8.71 ± 0.03	-0.68 ± 0.01	0.25 ± 0.05
NGC 1846	9.16	-0.68	0.12	3.1	0.30	8.80	0.85	2.9	9.28 (36)	9.15 ± 0.08	-0.72 ± 0.20	0.20 ± 0.16
NGC 1866	8.31	-1.68	0.36	2.2	0.00	8.31	0.00	2.2	8.31 (100)	8.31 ± 0.04	-1.73 ± 0.17	0.37 ± 0.10
NGC 1978	10.30	-1.68	0.53	2.3	0.01	10.28	0.09	2.3	10.30 (92)	10.14 ± 0.31	-1.57 ± 0.31	0.54 ± 0.15
NGC 2010	8.41	-2.28	0.18	2.4	0.02	8.47	0.18	2.4	8.41 (63)	8.42 ± 0.03	-2.22 ± 0.20	0.13 ± 0.08
NGC 2121	10.11	-1.68	0.81	5.0	0.02	10.18	0.15	5.0	10.30 (60)	9.97 ± 0.31	-1.48 ± 0.40	0.65 ± 0.28
NGC 2133	8.76	-2.28	0.17	2.5	0.01	8.77	0.13	2.4	8.86 (54)	8.67 ± 0.20	-1.81 ± 1.00	0.19 ± 0.11
NGC 2134	8.71	-2.28	0.04	1.9	0.07	8.78	0.22	1.8	8.81 (42)	8.62 ± 0.07	-2.04 ± 0.29	0.10 ± 0.09
NGC 2136	8.11	-1.68	0.51	2.3	0.03	8.24	0.38	2.3	8.21 (48)	8.10 ± 0.09	-1.45 ± 0.49	0.39 ± 0.13
NGC 2203	9.21	-0.68	0.37	3.0	0.22	9.07	0.79	2.6	9.30 (38)	9.21 ± 0.09	-0.68 ± 0.09	0.36 ± 0.07
NGC 2210	9.94	-2.28	0.36	2.5	0.60	8.90	1.66	2.1	6.54 (29)	9.88 ± 0.15	-2.18 ± 0.22	0.31 ± 0.12
NGC 2213	9.16	-0.68	0.22	2.3	0.16	9.05	0.45	2.1	9.28 (47)	9.16 ± 0.00	-0.68 ± 0.00	0.22 ± 0.05
NGC 2214	8.26	-2.28	0.00	2.3	0.20	8.21	0.54	2.2	8.36 (83)	8.12 ± 0.10	-1.86 ± 0.32	0.06 ± 0.05
NGC 2249	8.76	-0.68	0.30	2.2	0.05	8.70	0.23	2.1	8.76 (71)	8.76 ± 0.03	-0.68 ± 0.10	0.29 ± 0.06
47Tuc	9.89	-0.38	0.00	2.9	0.02	9.84	0.52	2.9	9.99 (23)	9.85 ± 0.04	-0.38 ± 0.00	0.07 ± 0.05
M 15	9.94	-2.28	0.19	2.5	1.58	8.41	1.66	1.6	6.52 (37)	9.94 ± 0.07	-2.28 ± 0.02	0.18 ± 0.06
M 79	9.68	-1.68	0.00	1.9	0.24	9.67	0.83	1.7	10.30 (30)	9.85 ± 0.23	-1.90 ± 0.29	0.02 ± 0.02
NGC 1851	10.03	-1.68	0.46	2.6	0.01	10.02	0.12	2.6	9.98 (50)	9.96 ± 0.05	-1.68 ± 0.00	0.52 ± 0.08

Table 8. Results for BBC00s models

	Single population fits					Multi population fits				Bayesian estimates		
Cluster (1)	$\log t$ (2)	$\log Z/Z_\odot$ (3)	A_V (4)	$\overline{\Delta}$ (5)	δ_m (6)	$\overline{\log t_m}$ (7)	σ_m (8)	$\overline{\Delta}_m$ (9)	$\log T_m$ (%) (10)	$\log t$ (11)	$\log Z/Z_\odot$ (12)	A_V (13)
NGC 411	9.11	-1.28	0.60	2.6	0.11	9.03	0.47	2.5	8.66 (28)	9.13 ± 0.06	-1.30 ± 0.09	0.58 ± 0.06
NGC 416	10.30	-1.68	0.16	2.0	0.08	10.02	0.71	2.0	10.29 (59)	10.13 ± 0.12	-1.68 ± 0.00	0.30 ± 0.12
NGC 419	9.11	-1.28	0.58	1.6	0.16	9.08	0.40	1.5	9.01 (27)	9.11 ± 0.01	-1.28 ± 0.01	0.57 ± 0.03
NGC 1651	9.34	-1.28	0.36	4.0	0.14	9.16	0.75	3.9	9.57 (34)	9.41 ± 0.13	-1.33 ± 0.19	0.41 ± 0.18
NGC 1754	10.22	-1.68	0.00	2.3	0.21	9.87	1.13	2.1	10.30 (49)	10.19 ± 0.04	-1.68 ± 0.00	0.04 ± 0.04
NGC 1783	9.51	-1.68	0.76	2.0	0.00	9.51	0.00	2.0	9.51 (100)	9.51 ± 0.02	-1.67 ± 0.06	0.76 ± 0.05
NGC 1795	9.36	-1.28	0.29	5.0	0.06	9.01	1.01	4.9	9.54 (38)	9.65 ± 0.35	-1.44 ± 0.22	0.39 ± 0.20
NGC 1806	9.28	-1.28	0.63	2.1	0.40	9.12	0.62	1.8	9.54 (25)	9.28 ± 0.02	-1.28 ± 0.05	0.63 ± 0.05
NGC 1818	7.40	-0.38	0.33	2.0	0.00	7.40	0.01	2.0	7.40 (76)	7.39 ± 0.03	-0.38 ± 0.00	0.35 ± 0.09
NGC 1831	8.71	-0.68	0.31	2.0	0.00	8.71	0.02	1.9	8.71 (90)	8.71 ± 0.02	-0.68 ± 0.00	0.30 ± 0.06
NGC 1846	9.26	-1.28	0.48	3.0	0.10	9.24	0.67	2.9	9.60 (28)	9.23 ± 0.06	-1.18 ± 0.23	0.48 ± 0.07
NGC 1866	8.31	-1.68	0.43	2.1	0.00	8.31	0.00	2.1	8.31 (100)	8.29 ± 0.05	-1.66 ± 0.14	0.44 ± 0.09
NGC 1978	9.48	-1.28	0.46	2.1	0.33	9.28	0.72	1.8	9.63 (43)	9.55 ± 0.26	-1.33 ± 0.13	0.49 ± 0.07
NGC 2010	8.36	-1.68	0.02	2.4	0.01	8.36	0.12	2.4	8.31 (56)	8.35 ± 0.02	-1.67 ± 0.09	0.06 ± 0.06
NGC 2121	10.17	-1.28	0.11	4.9	0.14	9.54	1.33	4.5	10.29 (19)	10.09 ± 0.22	-1.36 ± 0.17	0.31 ± 0.25
NGC 2133	8.31	0.00	0.27	2.4	0.00	8.30	0.04	2.4	8.31 (97)	8.48 ± 0.19	-0.89 ± 0.88	0.20 ± 0.11
NGC 2134	8.61	-1.68	0.00	1.8	0.02	8.64	0.16	1.8	8.76 (63)	8.56 ± 0.05	-1.68 ± 0.00	0.07 ± 0.06
NGC 2136	7.91	-0.68	0.37	2.3	0.01	7.92	0.02	2.3	7.91 (72)	7.93 ± 0.05	-0.73 ± 0.22	0.34 ± 0.09
NGC 2203	9.34	-1.28	0.65	2.8	0.12	9.46	0.76	2.6	9.57 (20)	9.35 ± 0.00	-1.27 ± 0.06	0.64 ± 0.07
NGC 2210	9.60	-1.68	0.16	2.7	0.63	9.43	1.16	2.0	10.30 (23)	9.61 ± 0.02	-1.68 ± 0.00	0.17 ± 0.07
NGC 2213	9.30	-1.28	0.53	2.3	0.08	9.30	0.48	2.2	9.16 (26)	9.30 ± 0.00	-1.28 ± 0.01	0.53 ± 0.05
NGC 2214	7.86	-0.68	0.00	2.1	0.04	7.82	0.42	2.1	7.91 (84)	7.98 ± 0.09	-1.22 ± 0.56	0.08 ± 0.07
NGC 2249	8.81	-0.68	0.28	2.3	0.13	8.67	0.39	2.1	8.66 (35)	8.78 ± 0.04	-0.83 ± 0.27	0.38 ± 0.12
47Tuc	9.48	0.00	0.00	3.1	0.09	9.42	0.66	3.0	9.54 (44)	9.77 ± 0.13	-0.32 ± 0.14	0.09 ± 0.07
M 15	9.63	-1.68	0.04	2.8	1.55	8.73	1.38	1.6	6.56 (23)	9.64 ± 0.02	-1.68 ± 0.00	0.07 ± 0.05
M 79	9.68	-1.68	0.04	1.9	0.25	9.78	0.73	1.6	10.30 (30)	9.67 ± 0.01	-1.68 ± 0.00	0.04 ± 0.03
NGC 1851	9.98	-1.68	0.55	2.6	0.04	10.05	0.16	2.6	9.95 (71)	9.96 ± 0.00	-1.68 ± 0.02	0.56 ± 0.07